Direct Force Measurements between Surfaces Coated with Hydrophobic Polymers in Aqueous Solutions and the Separation of Mixed Plastics by Flotation

Nini Ma

Thesis submitted to
the Faculty of the Virginia Tech in partial
fulfillment of the requirements for the degree of

Master of Science

in

Mining and Minerals Engineering

Roe-Hoan Yoon, Chair
Gregory T. Adel
Gerald H. Luttrell

Aug.27, 2008
Blacksburg, Virginia

Keywords: surface force, hydrophobic polymers, DLVO theory, froth flotation, contact angle, plastics recycling, flotation of plastics

Direct Force Measurements between Surfaces Coated with Hydrophobic Polymers in Aqueous Solutions and the Separation of Mixed Plastics by Flotation

Nini Ma

ABSTRACT

Froth floatation is an important process used in the mining industry for separating minerals from each other. The separation process is based on rendering a selected mineral hydrophobic using an appropriate hydrophobizing reagent (collector), so that it can selectively attach onto the surfaces of a rising stream of air bubbles. Thus, controlling the hydrophobicity of the minerals to be separated from each other is of critical importance in flotation. If one wishes to separate plastics from each other by flotation, however, it would be necessary to render a selected plastic hydrophilic and leave the others hydrophobic. In the present work, the possibility of separating common plastics from each other by flotation has been explored.

While water contact angle is the most widely used measure of the hydrophobicity of a solid, it does not give the information on the kinetics of flotation. Therefore, the forces acting between the surfaces coated with different hydrophobic polymers (or plastics) in water were measured using the Atomic Force Microscope (AFM). The results obtained with polystyrene, poly(methyl methacrylate) (PMMA), polypropylene (PP), and Teflon showed the existence of long-range attractive forces (or hydrophobic force) that cannot be explained by the classical DLVO theory. The surface force measurements were conducted in pure water and in solutions of surfactant (alkyltrimethylammonium chloride) and a salt (NaCl). In pure water, the attractive forces were much stronger than van der Waals force. In the presence of the surfactant and NaCl, the long-range attraction decreased with increasing concentration and the alkyl chain length.

A series of contact angle measurements were conducted to determine the hydrophobicity of polystyrene (PS), polyvinyl chlorite (PVC), and polymethylmethacrylate (PMMA) in the presence of different wetting agents (surfactants). The results show the possibility of separating plastics from each other by flotation, and a series of microflotation tests conducted on PS and PVC showed promising results.

TABLE OF CONTENTS

INDEX OF FIGURES AND TABLES

ACKNOWLEDGEMENTS

I would like to express my deepest appreciation to my advisor, Dr. Roe-Hoan Yoon, for his guidance, inspiration and support throughout the course of this work. Dr. Gerald Luttrell is also deeply acknowledged for teaching me in graduate classes and supporting my research. I also would like to thank Dr. Gregory T. Adel for his helpful suggestions.

Special thanks are directed to Dr. Jinhong Zhang for his training, instruction, guidance and inspiration in my research, and his help with AFM force measurement.

I would like to extend my thanks to the Center for Advanced Separation Technology and the U.S. Department of Energy for their financial support.

Sincere appreciations are extended to Jinming Zhang, Jialin Wang and Rayjia Wang for their friendship and support during the course of my studies at Virginia Tech.

Lastly, I express my deepest gratitude and appreciation to my dear parents, for their understanding, support and love.

I - INTRODUCTION

1.1 Hydrophobic Forces

In the mining industry, froth flotation is the most widely used method for separating fine particles. In this process, selected hydrophobic minerals are attached to air bubbles to be separated from hydrophilic particles. The control of particle hydrophobicity is thus of crucial importance for improving flotation performance. However, the exact nature of the mechanisms involved in hydrophobicity, especially the origin of forces between two hydrophobic surfaces in water, is still not completely understood.

In the early days, classical DLVO theory was used to predict the kinetics of coagulation and to describe interactions between particles. The DLVO theory considers two surface forces: the double-layer force and the van der Waals force. In 1961, Derjaguin and Dukhin [1] modeled flotation using these two surface forces. However, both the double-layer and the van der Waals forces are repulsive in most of the conditions encountered in flotation, which made it difficult to model fast and spontaneous flotation. The presence of an additional non-DLVO interaction was first recognized by Laskowski and Kitchener in 1969 [2]. They found that methylated and pure silica particles had practically the same ξ-potentials, and yet only the former floated while the latter did not, which led to the suggestion that a long-range "hydrophobic influence" may be responsible for the rupture of the wetting film, and thus, for the bubble-particle interactions in flotation. The authors suggested that the hydrophobic influence could be caused by the instability of the water structure in the vicinity of a hydrophobic surface. Later, Blake and Kitchener [3] showed that the thin film of water between a hydrophobic solid and an air bubble ruptures fast and spontaneously and that it does so at separation distances of about 64nm, which was much larger than predicted by the classical DLVO theory. These investigators suggested the presence of a "hydrophobic force" in wetting film between bubble-particle. The term *hydrophobic force* is now widely used to describe the long-range, non-DLVO attractive forces measured between macroscopic hydrophobic solid surfaces immersed in water.

The non-DLVO hydrophobic force was first measured experimentally in 1982 using the Surface Force Apparatus (SFA) by Israelachvili and Pashley [4]. The force was shown to decay exponentially in the 0-10 nm range with a decay length of 1 nm. The authors postulated that the force was related to the hydrophobic effect, which is widely used to explain mutual attraction between hydrophobic solutes (*e.g.* hydrocarbons) in water. Many other investigators conducted follow-up experiments and reported even longer-range of hydrophobic forces, whose decay lengths were shown to vary in the range of 10-30 nm.

When measuring hydrophobic forces, the adsorption of surfactants at the solid-liquid interface involves complex mechanisms and may introduce artifacts. Since the 1990's, direct force measurement between naturally hydrophobic polymer surfaces, without the use of surfactants, has become popular in the study of hydrophobic forces. However, the existence of hydrophobic forces remains controversial, since previous studies provide contradictory results. In 1993, Karaman *et al.* [5] measured the forces between polystyrene surfaces in water. The result showed that attractive forces pulled the surfaces into contact, from an initial separation distance as large as 30 nm. No further details regarding the nature of this attractive force were presented. In the same year, Li *et al.* [6] measured forces between 2 μm diameter polystyrene spheres in solutions using a Scanning Force Microscope. The results showed no long-range attraction, but only the existence of a repulsive electrostatic force. In 1994, Meagher and Craig [7] studied the effect of degassing on the surface force between polypropylene surfaces (θ = 90°-111 °) in NaCl solution, using an AFM. The authors postulated the existence an attractive force stronger than the van der Waals force both with and without degassing the solution. The jump distance, particularly significant before degassing, was measured to be as large as 21.0$\pm$5.2 nm, indicating the presence of the hydrophobic force. In 1999, no long-range hydrophobic attraction was found in the measurement performed by Schmitt *et al.* [8] on the surface between two fused polystyrene surfaces. In 2001, Vinogradova *et al.* [9] measured the interaction force between polystyrene surfaces and discovered a long-range attraction inconsistent with the DLVO theory. Considine *et al.* [10] investigated the force between polystyrene sphere and plate in aqueous media using an AFM. It was reported

that an attraction, much stronger than the van der Waals force, pulled the two spheres into contact with the initial separation distance from a quite long range (20-400 nm). The range of this strong attraction was found to decrease significantly after degassing.

Although much attention has been paid to the long-range attraction between hydrophobic surfaces in aqueous solutions, its origin still remains unclear. Two mechanisms have been proposed to explain the attractive forces between hydrophobic surfaces, including the popular nano-bubble hypothesis, which attributes the attraction to the capillary force caused by the coalescence of preexisting nano-bubbles as surfaces approach each other, and the charged-patch model, which uses the change of water structure near hydrophobic surfaces to account for the attractive force. Zhang *et al.* [11] observed and measured the presence of attractive forces between a glass sphere and a fused-silica plate in aqueous C_{18}TACl solutions using AFM. The magnitude of the attractive force was found to be much larger than the magnitude of the Van der Waals force, both in air-saturated and degassed solutions. The effect of dissolved gas on the hydrophobic attraction between surfactant-coated mica surfaces was studied by Meyer *et al.* [12] using SFA. Degassing was found to reduce the attraction range and to have virtually no effect within short range.

Both the above studies and the fact that no steps were detected on the surface force curve indicated that the nano-bubble hypothesis is inapplicable to the surfactant *in situ* adsorption system. This hypothesis, however, would require further investigation in the case of natural hydrophobic polymer surfaces, which exhibit high hydrophobicity (θ>80°).

The charged-patch model was proposed by Miklavic *et al.* [13], who studied long-range forces in high-concentration electrolyte solutions. In the framework of this model, it is suggested that "foreign" species in the solution may cause the breakdown of the water structure and thus decrease the long-range attraction. Zhang *et al.* [14] reported surface force measurements using an AFM with silica surfaces immersed in C_nTACl solutions in the absence of salt (n=12-18). These measured forces were in agreement with the charged-patch model. The results also showed that the long-range attractions first

increased with growing surfactant concentration, reaching a maximum at the point of charge neutralization (p.c.n.) and then decreased.

The main objective of the present investigation was to measure the surface forces between different plastics (hydrophobic polymers) immersed in water using an AFM. The measurements were conducted more systematically than reported previously in literature, and the results were analyzed quantitatively in view of the extended DLVO theory (Xu and Yoon, 1990, [15]).

1.2 Plastics Flotation

Despite a growing interest in recycling worldwide, a relatively small amount of plastic is recycled due to the lack of effective methods for separating different types of plastics from each other from a mixture. If one wishes to separate them by froth flotation, proper understanding of the surface properties of different plastics would be essential. Various wetting agents are used to modify the surface properties (hydrophobicity) of plastics. In the present work, water contact angles are used as the measure of surface hydrophobicity. Our research aims at controlling the hydrophobicity by using appropriate wetting agents and achieving the separation of mixed plastics by flotation.

During the past two decades, research in plastic flotation mainly focused on wetting plastics selectively by using various flotation depressants. Saitoh *et al.* [16] measured the water contact angles of various plastics such as polypropylene (PP), polyethylene (PE), polystyrene (PS), and polyvinyl chlorite (PVC), at different concentrations of a wetting agent (sodium lignosulfonate). In pure water, all plastics exhibit contact angles greater than 80^{o}, indicating strong hydrophobicity. The differences in hydrophobicity among these plastics are too small to allow separation by flotation. As the concentration of the wetting agent increases, however, the contact angles are reduced substantially and the difference in hydrophobicity is thus magnified. This phenomenon serves as a basis for separating plastics by flotation.

Many investigators showed that mixed plastics can be separated from each other by flotation if the surface properties are modified appropriately. Sisson [17] showed that in 2-15% NaOH (or KOH) and 0.005-0.1% NEODOL®91-6 (a non-ionic surfactant) solutions the contact angle of PET was decreased to below 25^{o}, while that of PVC remained above 45^{o}. Flotation separation under these conditions gave a 93.5% PVC recovery and a 97.5% PET recovery. Shibata *et al.* [18] developed a flowsheet for the flotation separation of a mixed plastic, in which POM and PVC were floated together by depressing PVC with 500 mg/l sodium lignosulfonate. Th POM was then floated from the POM/PC mixture by using 200 mg/t Saponin and 50 mg/l Aerosol OT to depress PC. Singh [19] separated PVC and POM successfully using appropriate wetting agents. Their results showed that sodium lignosulfonate was a good depressant for PVC while sorbitan monolaurate was good for POM. Drelich *et al.* [20] found that the hydrophobicity of PET was strongly altered by strong alkaline solutions of sodium hydroxide, while the hydrophobicity of PVC remained the same. The PET and PVC recoveries were 95 to 100%, respectively. Le Guern *et al.* [21, 22] studied the adsorption mechanism of lignosulphonate onto PVC and PET surfaces. Results showed that lignosulphonate could selectively interact with PET and render it hydrophilic. Also, the presence of divalent cations such as calcium could enhance the hydrophilization of PET through electrostatic bridge action between the lignosulphonate and the plastics. Both of them were negatively charged before the treatment. Shen *et al.* [23, 24] found that methyl cellulose can depress the flotation of PVC more readily than PET. The authors also investigated the floatability of seven plastics in the presence of an alkyl ethoxylated non-ionic surfactant (15-S-7, for example). The floatability was shown to decrease with addition of the surfactant. Floatability was depressed to a different extent for each plastic (POM < PVC < PMMA < PET < PC < ABS < PS). Dodbiba *et al.* [25] separated PET from both PET/ PE and PET/ PP mixtures using either 0.02 kg/m^3 dodecylamine acetate or polyvinyl alcohol. Basarova *et al.* [26] studied the wettability and floatability of PS in the presence of terpinol, polyethylene glycol dodecyl ether (PGDE), tannic acid, and calcium lignosulfonate. The results showed that at concentrations above 60 mg/l, PGDE increased the wettability of PS considerably while at concentrations below 20 mg/l, calcium lignosulfonate strongly

decreased the wettability. Tannic acid, on the other hand, with increasing concentration, decreased the floatability linearly.

The froth flotation technique is based on the selective adherence of gas bubbles onto the particles to be separated. For this purpose, a sufficient difference in wettability is required between these particles. Since plastics are naturally hydrophobic, selective wetting of each component is necessary for the separation by flotation. However, a comprehensive understanding of the wetting phenomena involved has not been established yet. Thus, the wetting action of a given surfactant during flotation cannot be predicted.

1.3 Research Layout

This work was devoted to the experimental investigation of surface forces and wettability of plastics in the presence of various wetting agents. The overall objective was to better understand the origin of hydrophobic force and identify the conditions under which different plastics (or hydrophobic polymers) can be separated from each other. In Chapter 2, the results of the AFM surface force measurements conducted between PS, PMMA, PP and Teflon surfaces in pure water and solutions of different surfactants and electrolytes. Chapter 3 describes an experimental study aimed at finding more efficient wetting agents for the separation of PS and PVC by flotation.

II - HYDROPHOBIC FORCES BETWEEN PLASTIC SURFACES IN AQUEOUS SOLUTIONS

The surface forces acting between hydrophobic surfaces play an important role in flotation. In the froth floatation process, the efficiency of separation is largely determined by the interaction between hydrophobic air bubbles and hydrophobic particles. Therefore, it has become increasingly important to achieve a better understanding of the origin of hydrophobic forces. The non-DLVO theory, which takes into account the hydrophobic force, the van der Waals force and the electrostatic force, has been recently applied to explain the phenomena involving hydrophobic interaction. There have been more and more evidences indicating that the non-DLVO theory is a more thorough theory than the classical DLVO theory, for which numerous discrepancies with experiment results have been found.

Plastics are ideal materials to study the hydrophobic force, because they are naturally hydrophobic, and they don't introduce the complexity arising from surfactant adsorption. The existence of hydrophobic attraction between hydrophobic plastic surfaces has been investigated by many researchers. In 1993, Karaman *et al.* [5] measured the forces between polystyrene surfaces in water, and recorded a jump-in distance as large as 30 nm. Li *et al.* [6], in 1993 also measured forces between polystyrene surfaces but observed no long-range attraction force. In 1999, Schmitt *et al.* [8] performed surface force measurement between two fused polystyrene surfaces, but their results showed no long-range hydrophobic attraction. In the same year, Considine [10] observed a much stronger attraction force than the van der Waals fore, with a jump-in distance from a quite long range (20-400 nm), between different pairs of polystyrene spheres. In 2001, Vinogradoca *et al.* [9] tested the same plastic, and a long-range attraction was also observed.

Force measurements have also been conducted with Teflon and other plastics. In 1994, Meager and Craig [7], using an AFM, investigated the hydrophobic interaction between polypropylene surfaces in NaCl solution. A 30 nm range where they observed the attractive forces was found in solutions both with and without degassing. Nalaskowski et al. [27] measured forces between a polyethylene sphere and a polyethylene surface in de-

aerated and aerated water. A long-range attractive force between hydrophobic polyethylene surface and sphere was observed.

The Teflon has a very high contact angle (θ=110°). In 1999, Considine et al. [28] measured the force between a micron-sized colloidal sphere and a flat plate, both coated with a copolymer of perfluoro (2, 2-dimethyl-1, 3-sioxole) and Teflon AF 1600. It was shown that the surfaces experienced a very strong attraction as two surfaces contact each other. The jump-in distance was about 500 nm in water. In 2005, Hallam et al. [29] also observed a long-ranged attraction between hydrophobic amorphous fluoropolymer surfaces. They found that the range of the attraction and its attraction decreased in de-aerated water as compared to normal, aerated water. However, the range and the strength of the attraction in deaerated water remained significantly greater than those of the van der Waals attraction for this system.

In this chapter, the results of the hydrophobic force measured between various hydrophobic polymer-coated surfaces, which included PS, PMMA, PP and Teflon were studied. The measurements were conducted using an Atomic force microscope in water and surfactant solutions. The relationship between surface forces and contact angles has been studied. The objective of this study was to study the nature of hydrophobic forces.

2.1 Materials and Experiments

2.1.1 Plastic Spheres

Polystyrene (PS) spheres of 10-15 μm in diameter were purchased from Polysciences, Inc., Warrington, PA. They were soaked and settled in ethanol for 1 hour. The suspension was withdrawn to remove possible organic contaminants. This procedure was repeated three times. Polymethyl methacrylate (PMMA) spheres of 19.8 μm in diameter were provided by Corpuscular Inc., New York. They were cleaned in the same manner as described for polystyrene. PP and Teflon spheres were formed directly on the tip of a cantilever by melting a small amount of powder at 130 ℃ and 190 ℃. The spheres were then stored in a N_2 atmosphere until use (no longer than 3-4 days).

2.1.2 Synthesis of PS, PMMA and PP Substrates Through Spin-coating

Silicon wafers were provided by Sumco, Oregon. They were boiled in a freshly prepared solution of NH_4OH:H_2O_2:H_2O (1:1:5 by volume) for about 1.5 hour at 110 ± 5^oC to clean their surface. The wafers were then rinsed thoroughly with a large amount of Milli-Q water, and dried by blowing pure nitrogen over the surface. The plates were then heated in a piranha solution, a solution of concentrated H_2SO_4 and H_2O_2 (7:3 by volume), for at least 60 minutes, rinsed thoroughly with Milli-Q water, and then dried with nitrogen again. The plates were further submerged in an HF solution for 3 minutes and in an ammonium fluoride solution for about 1 minute. After being rinsed with water and dried with nitrogen, the plates were immediately spin-coated.

PS, PMMA and PP powders were dissolved in toluene to get 0.3% solutions for spin coating on the surface of silicon wafer.

Teflon substrates were prepared by melting the Teflon solid layer which was evenly placed on the cleaned silicon wafer surface and heated to 190 ℃. A nitrogen stream was used to remove remaining flakes.

2.1.3 Water and Surfactant Solutions

Nanopure water was obtained by using the Nanopure III (Barnstead IA) water purification system. The conductivity of the water was 18.2 MΩ/cm at 25°C and the surface tension was 72.5 mN/m at 22 ℃. Extra purging with ultra-pure nitrogen gas, to exclude atmospheric CO_2, has not been used here. Thus, the pH of the solutions was within the 5.8-6.0 range. Tetradecyltrimetylammonium chloride (C_{14}TACl), hexadecyltrimetylammonium chloride (C_{16}TACl) and octadecyltrimetylammonium chloride (C_{18}TACl) were provided by TCI, with purity greater than 97%. These surfactants were used for surface force measurements without further purification. Solutions of low surfactant concentrations were prepared in containers with volumes of at least 100 mL to prevent significant depletion of surfactant *via* adsorption onto the glass walls.

2.1.4 Surface Force Measurements on PS Surface

A Digital Instrument Nanoscope III (Veeco, CA) atomic force microscope (AFM) was used for surface force measurements [30, 31]. All experiments were performed at room temperature (22 ± 1^{o}C). Silicon dLever cantilevers and silicon-nitride NP-20 cantilevers were purchased for Veeco, CA. The cantilevers were calibrated using an adapted version of the Resonant Frequency Technique [32], which limits the calibration errors up to ±7%. A plastic sphere was attached on the tip of a cantilever spring so that the surface force measurement could be measured using the sphere-plate geometry. EPON 1004 resin (Shell Chemical Co.) was used to attach the spheres (10-15μm in diameter as measured by a microscope) onto cantilevers. The force measurements were conducted at different surfactant concentrations. The concentrations were controlled by adding more additional surfactant incrementally. At a given surfactant concentration, the system was equilibrated for 30 minutes before taking the measurements. No efforts were made to exclude the air from dissolving into the solution.

2.1.5 Contact Angle Measurement

The hydrophobicity of plastics (or silicon wafer coated with different hydrophobic polymers) was characterized by means of the water contact angles measured using the cessile drop technique. For each measurement, a drop of pure water was placed onto a plastic-coated silicon wafer, and the contact angles were measured using a goniometer. The results reported in this work were averages of over five such measurements.

The contact angles of the plastics were also measured in solutions of surfactants and electrolytes. In this case, the contact angles were measured using the captive bubble technique. In this method, a solid sample was immersed in a solution, and an air bubble formed at the end of a hypodermic needle was brought in contact with the solid surface sample from below. The contact angle was defined as the angle between a line tangent to the bubble and the surface of the solid sample, as shown in Figure 2.1.

2.1.6 Zeta-potential Measurement

The plastic spheres used for the AFM force measurements were used to measure the ξ-potentials at the solid-liquid interface. The measurements were conducted using the Zetanano series laser meter. The reported results were averaged over six independent measurements. 0.5g/l solution was prepared and ultrasonication was applied for 30 min to remove air bubble and breakup agglomerates.

2.2 Results and Discussion

2.2.1 AFM Image

Figure 2.2.a-c shows the AFM images of a silicon wafer surface coated with PS, PMMA and PP. The coating was prepared using the spin-coating as described in 2.1.2. The image represents the magnification of a 5 x 5 μm section of the surface, and its morphology is represented by color scaling. As shown the maximum peak-valley distance was approximately 1.8 nm, indicating that the spin-coated surface was smooth enough for surface force measurement.

2.2.2 Zeta-potential

The zeta-potentials of PS, PMMA and PP were obtained by means of the electrophoresis technique. The values of these potentials were found to be -30 mV, -67 mV and -80 mV, respectively, in water at pH = 6.0. Teflon zeta-potential data was not available due to the high hydrophobicity of Teflon and it was hard to get the suspension solution which was required for the measurement. The zeta potentials as a function of pH were also shown in Figure 2.3.

2.2.3 Surface Forces Measured in Nanopure Water

Figure 2.4 shows the results of the AFM force measurements conducted between polystyrene (PS) sphere and plate in water at neutral pH. The squares represent the experimental data, and the solid line represents a fit to the classical DLVO theory.

According to this theory, the total surface force (F_t) should be the sum of the electrostatic force (F_e) and the van der Waals dispersion force (F_d) as follows:

$$F_t = F_e + F_d, \tag{1}$$

in which

$$F_d = -\frac{RA_{131}}{6H^3}, \tag{2}$$

where R is the radius of the colloidal probe, A_{131} the Hamaker constant, and H is the closest separation distance between two macroscopic surfaces. The fit was made with A_{131} (Hamaker constant) =1.3x10^{-20} J [33] and ψ_0 (double-layer potential) = -30mV. As shown in Figure 2.3, two surfaces jumped into contact at 19.5 nm, which was substantially larger than what the DLVO theory predicted. This finding suggests that there may be additional attractive force other than the van der Waals force.

Figure 2.5 shows the same experimental results fitted to the DLVO theory (Eq. (1)) extended to include the hydrophobic force (F_h), as follows:

$$F_t = F_e + F_d + F_h, \tag{3}$$

in addition to the electrostatic and van der Waals forces. The hydrophobic force may be represented by the following expression:

$$F_h = RC\exp\left(-\frac{H}{D}\right), \tag{4}$$

where R is the radius of the sphere of the colloidal probe, H the closest separation distance between the surface of the sphere and the flat surface, and C and D are fitting parameters. The constant D is referred to as decay length, and the constant C is related to the interfacial tension between solid and liquid. The hydrophobic force curve shown in Figure 2.5 was obtained with C = 1.0 mN/m and D = 4.4 nm. The water contact angle measured using the sessile drop technique was 76°. The figure clearly shows that the

extended DLVO theory (Eq. (3)) can predict the jump-in distance better than the classical DLVO theory (Eq. (1)).

Figure 2.6 shows the results of the AFM force measurements conducted between a polymethyl methacrylate (PMMA) sphere and a silicon wafer coated with PMMA in water at the natural (*i.e.* unadjusted) pH. The solid line represents the DLVO fit of the data with $A_{131} = 1.05 \times 10^{-20}$ J [24] and ψ_0 = -68mV. The fit is not very good, as the theory predicts that the two surfaces should jump into contact at 6 nm, while it actually occurs at 24 nm. The large discrepancy suggests that additional attractive forces must be present between the hydrophobic surfaces. Therefore, the experimental data were fitted to the extended DLVO theory with C = 3.0 mN/m and D = 4 nm, as shown in Figure 2.7. The fit based on the recognition of the hydrophobic force was much better. The sessile drop contact angle of the PMMA plate was 72 °.

Figure 2.8 shows the results of the AFM force measurements conducted between a polypropylene (PP) sphere and a PP-coated silicon wafer plate in Nanopure water at a neutral pH. Contact angle of the PP-coated surface was 98^o as measured by the sessile bubble technique. The solid line represents the experimental data fitted to the DLVO theory with $A_{131} = 6.0 \times 10^{-20}$ J [35] and ψ_0 = -82.4mV. The DLVO theory predicts that the two surfaces should jump into contact at 5 nm, whereas the jump actually occurs at 28 nm. This large discrepancy again suggests an additional attraction causing the jump at such a large distance. Therefore, the experimental data was fitted to the extended DLVO theory (Eq. (3)) with C = 3.1 mN/m and D = 7.6 nm, as shown in Figure 2.9.

Table 2.1 summarizes the data presented in Figures 2.4-2.9. According to the equilibrium sessile drop contact angle (θ) data, PP is most hydrophobic, followed by PS and then PMMA. It is found that the decay length (D) follows the same order. The difference in θ is the largest between PP and PMMA. It is also found that these two polymers show the largest difference in D also.

Figure 2.10 shows the AFM force measurements conducted between a Teflon sphere and a Teflon-coated plate as described in 2.1.2. in Nanopure water at a neutral pH. With the sessile drop technique, the contact angle of the Teflon surface was measured to be 110^{o}. In Figure 2.10, the experimental data fitted to the DLVO theory with A_{131} = 3.59×10^{-21} J [27] is represented by the solid line. As discussed above, the two surfaces are predicted to jump into contact at 6 nm according to the DLVO theory. However, the jump actually occurs at 30 nm as shown in Figure 2.11. This discrepancy suggests the existence of an additional attraction between the two hydrophobic surfaces. Figure 2.11 also demonstrates that the experimental data is better fitted to the extended DLVO theory with C = 3.0 mN/m and D = 5.6 nm. However, although Teflon has the largest contact angle among these four plastics, the amplitude of its hydrophobic forces is not the greatest. This may be due to the roughness of Teflon, which could yield to an underestimation of the measured forces. The high potential of Teflon could also be a reason that the hydrophobic force appear to be small.

2.2.4 Surface Forces Measured in Surfactant Solutions

Figure 2.12 shows the AFM surface force measurements conducted between a PS sphere and a PS-coated silicon wafer surface in the presence of different concentrations of a cationic surfactant (C_{14}TACl). At low concentrations, *i.e.*, $8x10^{-5}$ and $1x10^{-4}$ M, the surface force decreased, due to both charge neutralization and increase in hydrophobic force. Since PS is negatively charged at neutral pH, the cationic surfactant can adsorb on the PS surface and thus increase the hydrophobicity of PS. The contact angle increased as the concentration was raised from $8x10^{-5}$ to $1x10^{-4}$ M, as shown in Table 2.2. These observations suggest that the cationic surfactant adsorbs with a normal mode of orientation, *i.e.* the polar head group being in contact with the PS surface.

Several authors [36-39] have shown that the attractive forces measured between hydrophobic surfaces reach a maximum as the surfactant's concentration gets close to the point of charge neutralization (p.c.n.). The p.c.n. is defined as the concentration, at which the surface charge of the substrate is neutralized by the adsorption of the cationic surfactant. For the F/R versus H curves shown in Figure 2.12, the p.c.n. corresponding to

the PS-C_{14}TACl system is approximately situated at 1×10^{-4} M. At this concentration, the attractive force reached a maximum. At the p.c.n., most negative sites are occupied by the $C_{14}TA^{+}$ ions, forming hemi-micelles in which the hydrocarbon tails of the adsorbed surfactant molecules are closely packed.

At 5×10^{-4}M C_{14}TACl, additional $C_{14}TA^{+}$ ions would adsorb on the substrate surface, but with inverse orientation. Such an orientation is favored, because it requires the least amount of energy to insert additional surfactant molecules into the adsorption layer with their polar heads furthest apart from each other. The inverse orientation exposes the head groups toward the aqueous phase and, hence, causes the surface to be less hydrophobic. Therefore, the decrease in attractive force at the higher concentration can be attributed to this phenomenon. The mechanism of inverse orientation is illustrated in Figure 2.19. Table 2.2 shows that the contact angle decreases to 78^{o} as the C_{14}TACl concentration was further increased to $5x10^{-4}$ M most probably due to inverse orientation. The additional surfactant present in the second-layer of adsorbed species not only reduce the contact angle but also increase the negative surface charge, both of which causing the surface force to be repulsive as shown in Figure 2.12.

Figure 2.13 shows the results obtained with a longer-chain homologue, C_{16}TACl. At 1×10^{-5}M C_{16}TACl, a very long-ranged and net-attractive force was observed. The strongest attractive force was measured for a concentration of 3×10^{-5}M C_{16}TACl. Thus, this concentration may be close to the p.c.n. of the PS-C_{16}TACl system. This value is significantly lower than that observed for the shorter chain homologues. The most interesting aspect of the data shown in Figure 2.13 is that the C-16 surfactant gives much stronger and longer-range attractive forces than those observed for the shorter chain homologues. With C_{16}TACl, net attractive forces were observed at separations as large as 60nm.

Figure 2.14 shows the results obtained with C_{18}TACl. The data show that the C-18 surfactant gave much stronger and longer-range attractive forces than those observed for the shorter chain homologues. At 5×10^{-6} M C_{18}TACl, a very long-ranged and net-

attractive force was observed for a separation distance as large as 65 nm. When the concentration was raised to 2×10^{-5} M C_{18}TACl, the attractive force became much stronger at a separation distance as large as 120 nm.

Figure 2.15 shows the results of the AFM surface force measurements conducted between a PS sphere and a PS-coated silicon wafer surface in a 0.1% sodium lignosulfonate solution. As shown in the figure, the surface forces measured with this anionic surfactant increased drastically and became much more repulsive in the presence of the anionic surfactant. At this concentration, the contact angle decreased sharply from $\theta = 74.4^{o}$ to 32.2^{o}. The decrease in contact angle and the increase in repulsive surface forces are most probably due to the inverse orientation of the anionic surfactant, *i.e.* adsorption with the hydrocarbon chains in contact with the PS surface and the anionic polar heads heading toward the aqueous phase.

Figure 2.16 shows the AFM surface force measurements conducted between a PMMA sphere and a PMMA-coated silicon wafer surface in the presence of different concentrations of a cationic surfactant (C_{14}TACl). At 8×10^{-5}M C_{14}TACl, a very long-ranged and net-attractive force was observed. When the concentration was raised to 1×10^{-4} M, the attractive force reached its maximum. Thus, the p.c.n. of the PMMA-coated silicon wafer-C_{14}TACl system was approximately 1×10^{-4} M, which is the same as for the PS-coated silicon wafer-C_{14}TACl system. As the concentration was further increased to $5x10^{-4}$ M, the cationic surfactant adsorbed with an inverse orientation. The inverse orientation further increases the positive charge of the surface and at the same time decreases the hydrophobicity, which is consistent with the result shown in Table 2.2, where the contact angle is shown to decrease from 72 °to 67^{o}, and the results shown in Figure 2.16, where the surface force becomes repulsive.

2.2.5 Surface Forces Measured in Salt Solution

Figure 2.17 shows the surface forces measured between a PMMA sphere and a PMMA-coated silicon wafer substrate immersed in salt (NaCl) solutions. When the salt concentration was increased from $1x10^{-3}$ M to $6x10^{-3}$ M, the measured forces changed

from repulsive to attractive. At $1x10^{-3}$ M, a long-range repulsive force was observed. However, the two hydrophobic surfaces jumped into contact at approximately 9 nm, which was considerably larger than predicted by the classical DLVO theory. Thus, the hydrophobic force was still there despite the fact that the measured force was net repulsive. At $3x10^{-3}$ M NaCl, the measured force was net attractive due to the reduction of the double-layer force. At $6x10^{-3}$ M, the double-layer force was further reduced and the two surfaces jumped into contact at a separation as large as 25 nm. These results indicate that the hydrophobic force was still present in the presence of $1x10^{-3}$ to $6x10^{-3}$ M NaCl. The D value was listed in Table 2.3 after eDLVO calculation.

Figure 2.18 shows the surface forces measured between a PP sphere and a PP-coated silicon wafer plate immersed in a 10^{-3} M NaCl solution. The results are similar to those obtained with the PMMA surfaces. The force measured in pure water was net repulsive due to a high surface charge. Yet, the two surfaces jumped into contact at approximately 30 nm, due to a strong hydrophobic force with a decay length (D) of 7.6 nm. At $1x10^{-3}$ M NaCl, the repulsive force disappeared, and the two hydrophobic surfaces jumped into contact at approximately 13 nm, indicating the presence of a strong hydrophobic force. The decay length was 8.1 nm, indicating that the presence of NaCl did not affect the hydrophobic force significantly.

2.3 Summary

An atomic force microscope (AFM) was used to measure the surface forces between PS, PMMA PP and Teflon surfaces in pure water and in different concentrations of surfactant and salt (NaCl) solutions. The forces measured in pure water were net repulsive due to the high surface charges, as indicated by their ς-potentials: -30 mV for PS, -67 mV for PMMA, and -80 mV for PP. Nevertheless, two hydrophobic surfaces jump into contact at separation distances much larger than predicted by the classical DLVO theory. The discrepancy can be attributed to the presence of the long-range hydrophobic force between the symmetric PS, PMMA and PP surfaces. In pure water, the hydrophobic forces decrease in the order of PP, PMMA and PS. In the presence of NaCl,

the repulsive double-layer force is decreased, and net attractive forces are observed due to the hydrophobic force.

The surface forces were also measured in the presence of a cationic (C_{14}TACl) and anionic (sodium lignosulfonate) surfactant. In the presence of the former, the hydrophobic force becomes stronger with increasing surfactant concentration due to the adsorption of the cationic surfactant with a normal mode of orientation, i.e., the head group in contact with the surface and the hydrocarbon tail protruding into the aqueous phase. As the surfactant concentration was increased beyond the p.c.n., the cationic surfactant begins to adsorb with inverse orientation and render the surface less hydrophobic. As a result the hydrophobic force becomes weaker. The surface forces measured with C_{16}- and C_{18}-TACl homologues showed the same trend as C_{14}TACl except that the hydrophobic forces measured at a given surfactant concentration was lower. In the presence of the anionic surfactant, the measured surface force becomes much more repulsive due to the inverse orientation of the surfactant molecules on the hydrophobic surface.

2.4 Figures and Tables

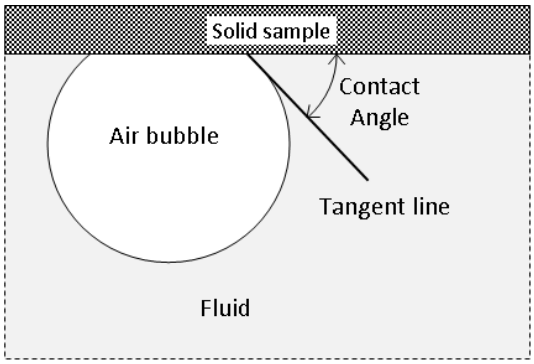

Figure 2.1 *Schematic representation of the captive bubble technique.*

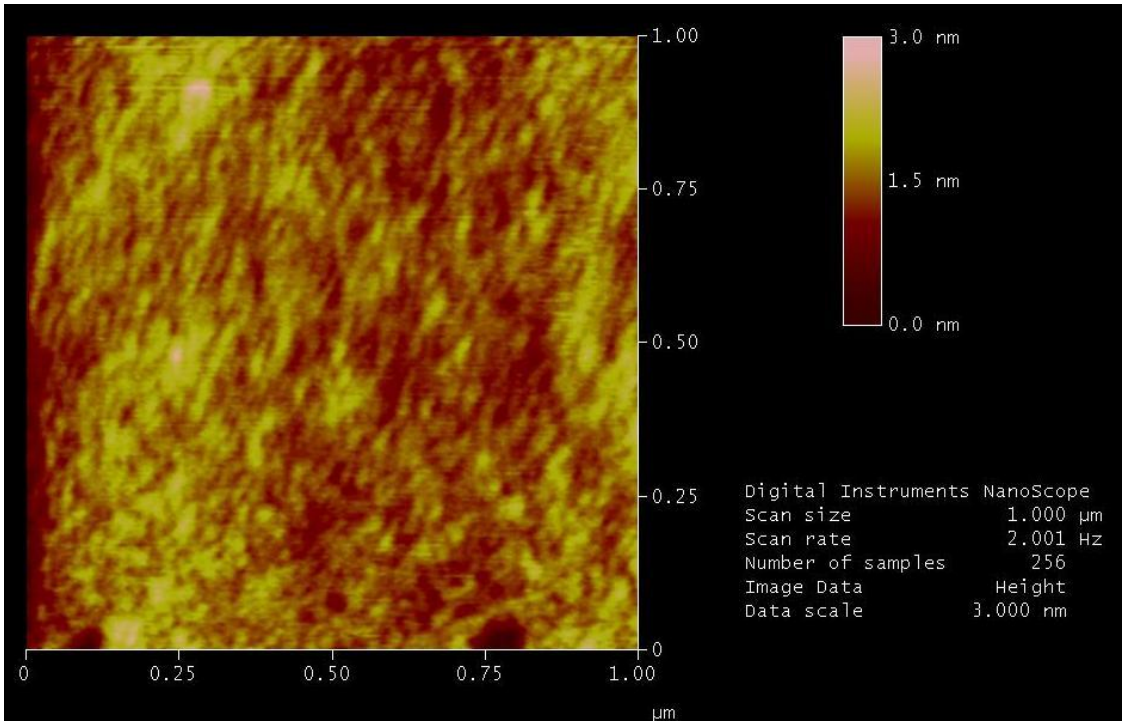

Figure 2.2.a *AFM image of PS substrate immersed in water. The scale of the image is 5 × 5 µm. The scale bar on the right side gives height information.*

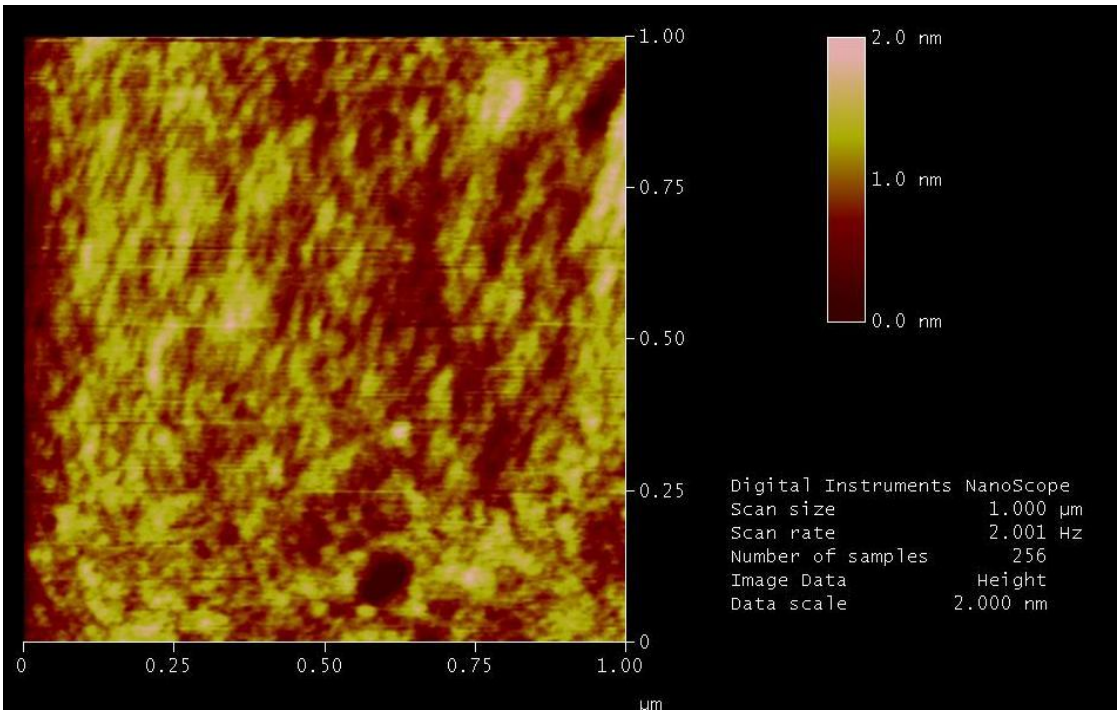

Figure 2.2.b *AFM image of PMMA substrate immersed in water. The scale of the image is 5 × 5 µm. The scale bar on the right side gives height information.*

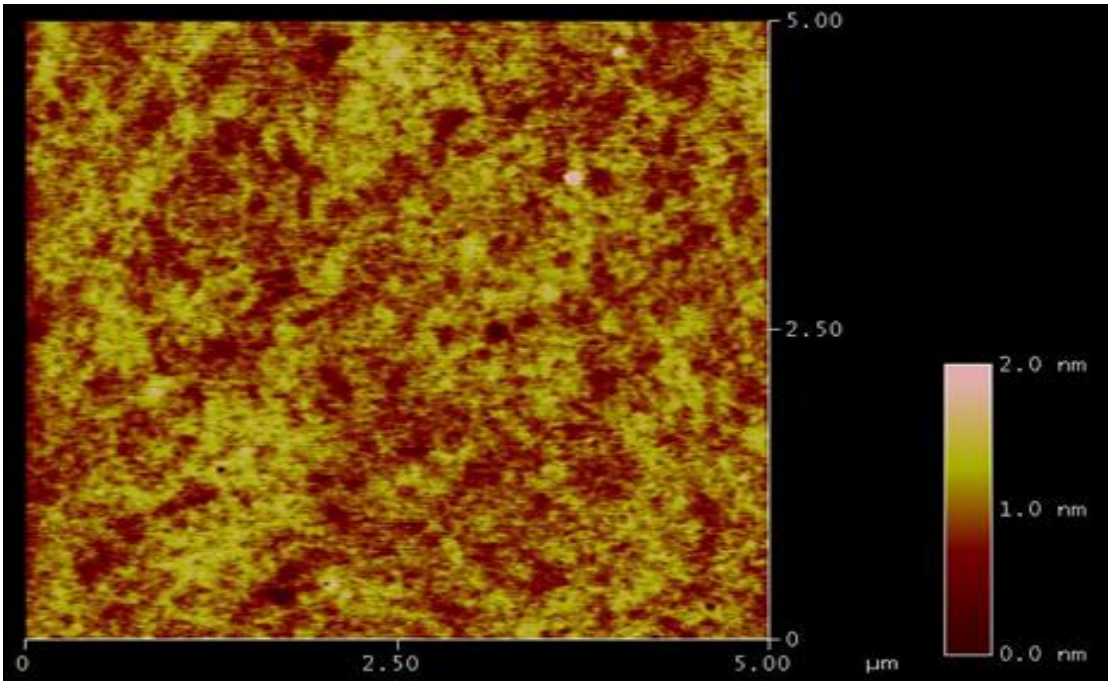

Figure 2.2.c *AFM image of PP substrate immersed in water. The scale of the image is 5 × 5 µm. The scale bar on the right side gives height information.*

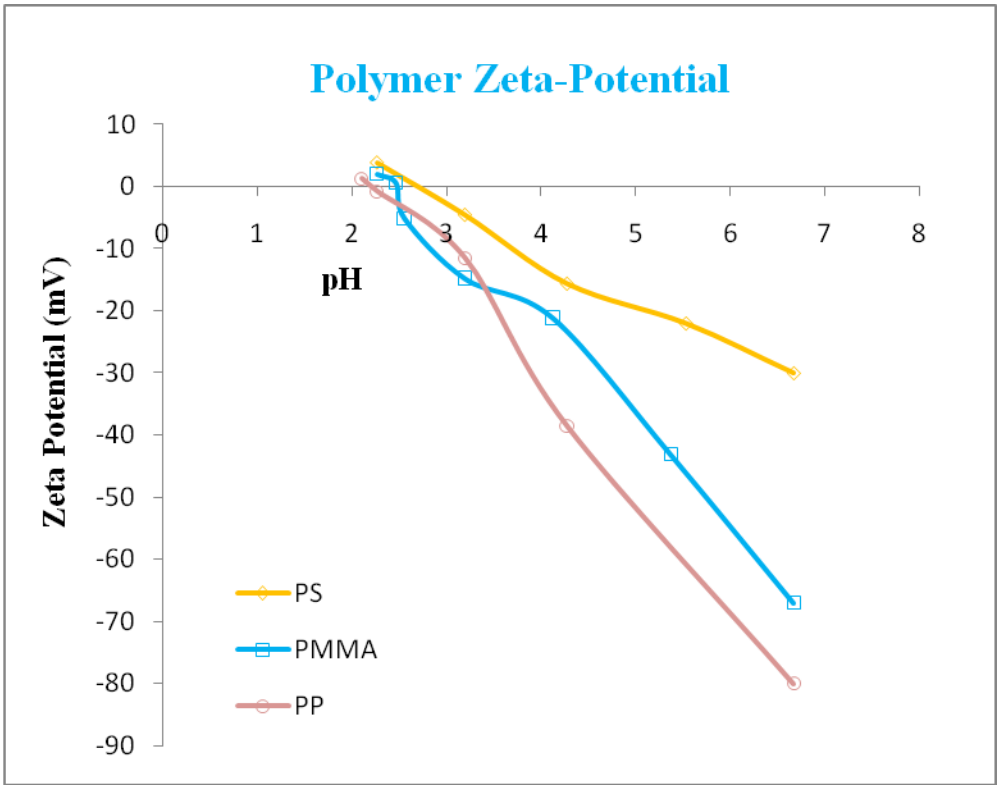

Figure 2.3 *Zeta-potential value of PS, PMMA and PP measured at different pH. For PS, at p.c.n., pH = 2.73 and zeta-potential value at natural pH is -30mV. For PMMA, at p.c.n., pH = 2.48 and zeta-potential value at natural pH is -67mV. For PP, at p.c.n., pH = 2.20 and zeta-potential value at natural pH is -80mV.*

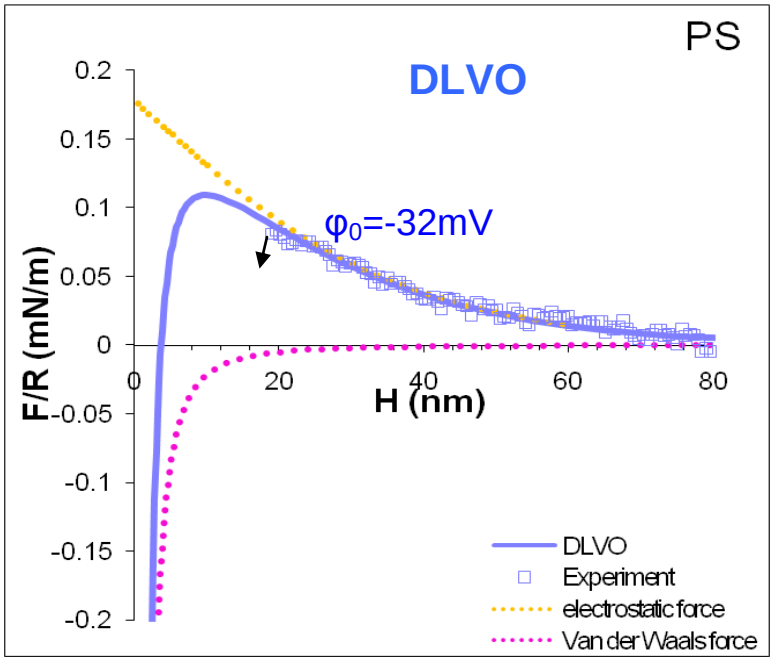

Figure 2.4 *AFM force measurements conducted between polystyrene (PS) sphere and plate in water at neutral pH: A_{131}=1.3x10^{-20} J; ξ=-30 mV; φ_0=-32 mV: θ=76°.*

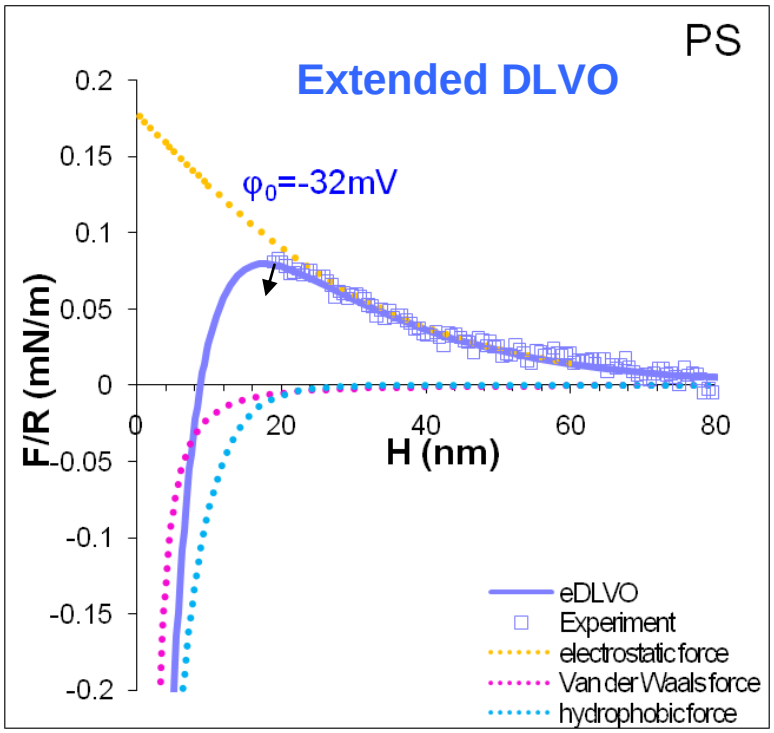

Figure 2.5 *AFM force measurements conducted between polystyrene (PS) sphere and plate in water at neutral pH: C=1.0 mN/m and D=4.4 nm; A_{131}=1.3x10-20 J; ξ =-30mV; φ_0 =-32mV; θ=76^o.*

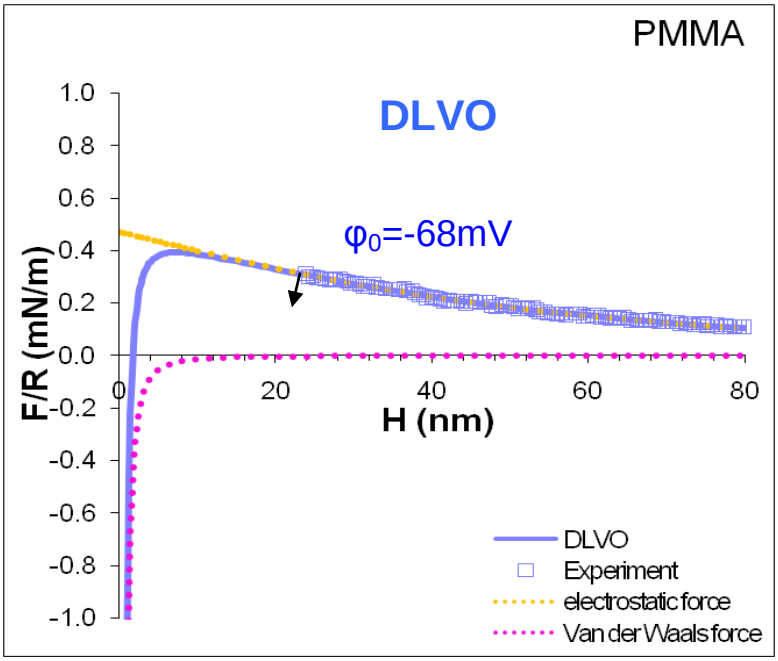

Figure 2.6 *AFM force measurements conducted between a polymethyl methacrylate (PMMA) sphere and plate in water at a neutral pH:* A_{131}*=* 8.0×10^{-21} *J;* ξ*= -67mV;* φ_0*=-68mV;* θ*=72°.*

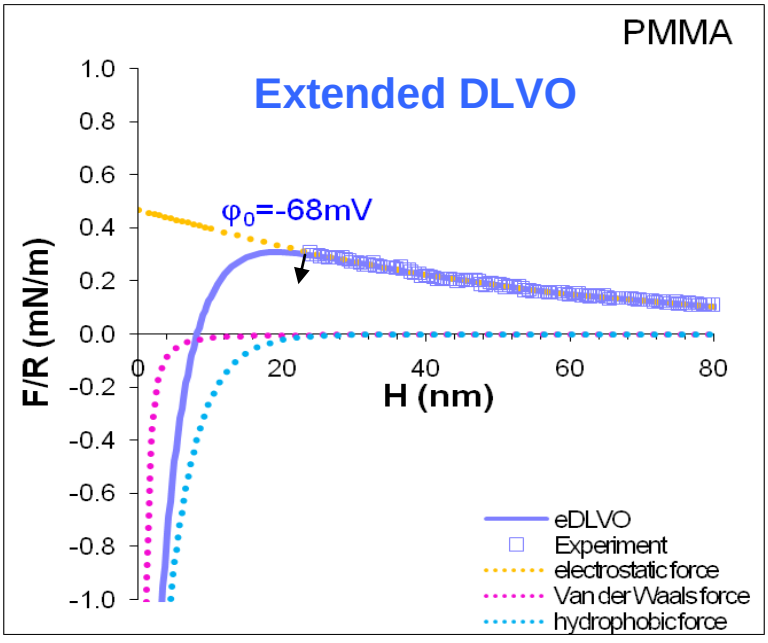

Figure 2.7 *AFM force measurements conducted between a polymethyl methacrylate (PMMA) sphere and plate in water at a neutral pH: C=3.0 mN/m and D=4.0 nm;* A_{131} *=* 8.0×10^{-21} *J;* ξ*=-67mV;* φ_0*= -68mV;* θ*=72.*^{o}

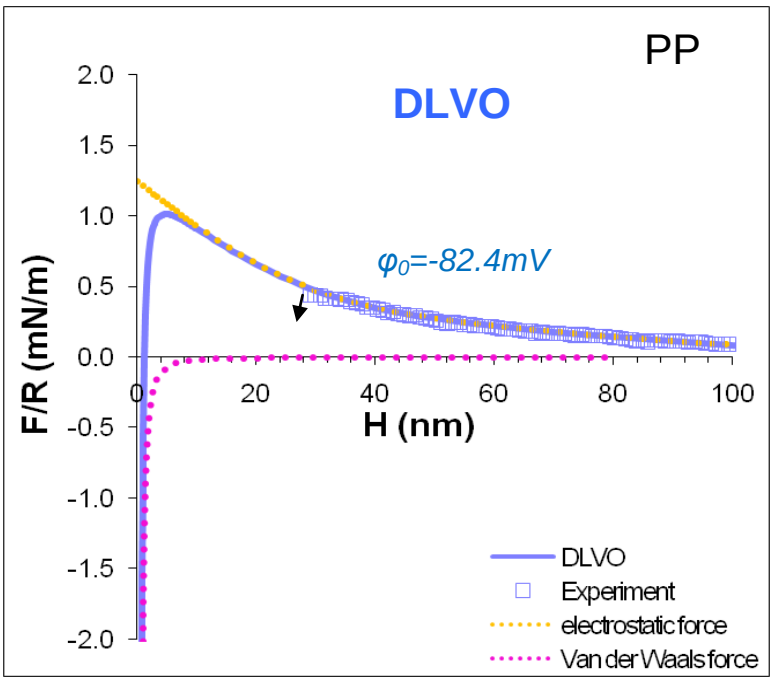

Figure 2.8 *AFM force measurements conducted between a polypropylene (PP) sphere and plate in water at a neutral pH: $A_{131}=1.05\times10^{-20}$ J; ξ=-80 mV; φ_0 =-82.4 mV; θ=98°.*

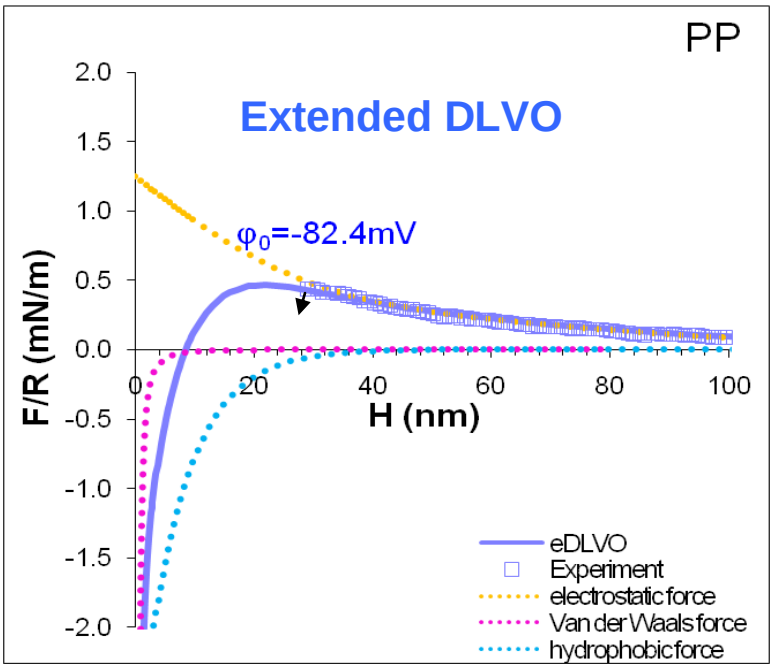

Figure 2.9 *AFM force measurements conducted between a polypropylene (PP) sphere and plate in water at a neutral pH: C =3.1 mN/m and D=7.6 nm; $A_{131}=1.05\times10^{-20}$ J; ξ=-80 mV; φ_0=-82.4mV; θ=98°.*

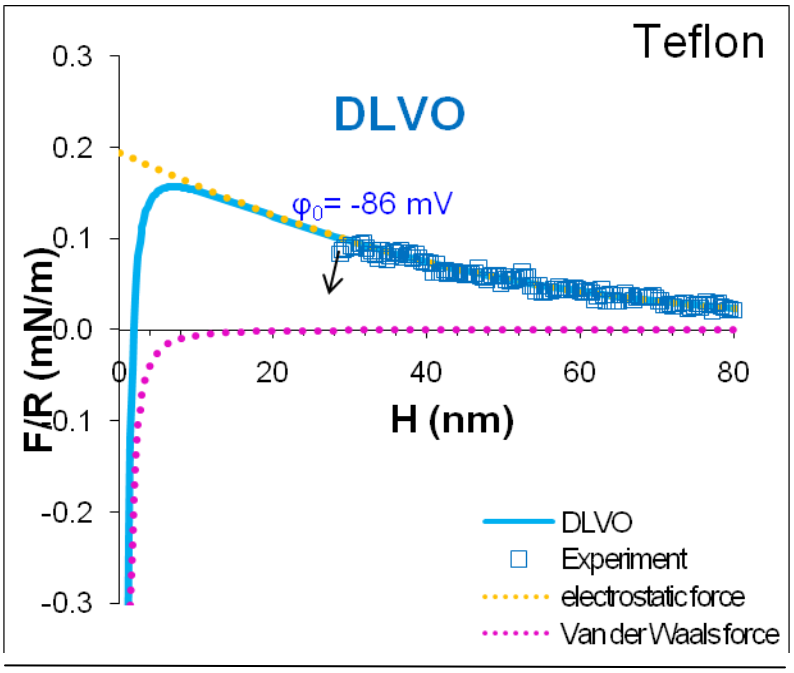

Figure 2.10 *AFM force measurements conducted between a Teflon sphere and plate in water at a neutral pH: $A_{131}=3.59\times10^{-21}$ J; $\varphi_0=-86$ mV; $\theta=110$ °.*

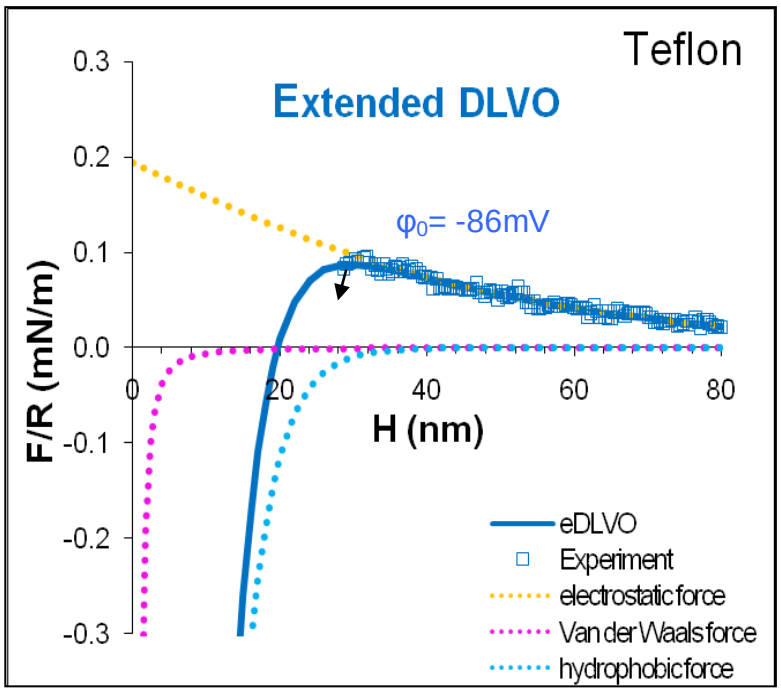

Figure 2.11 *AFM force measurements conducted between a Teflon sphere and plate in water at a neutral pH: C=3.0 mN/m and D=5.6 nm; $A_{131}= 3.59\times10^{-21}$ J; $\varphi_0= -86$mV; $\theta=110^{o}$.*

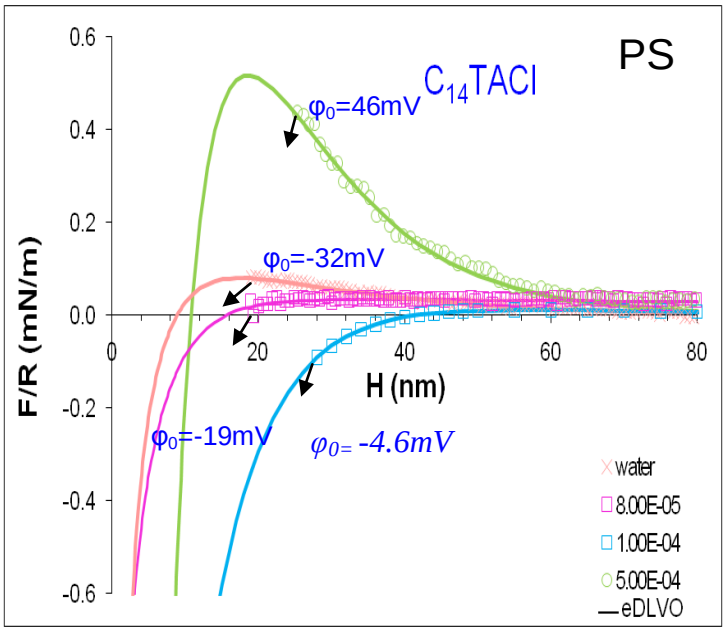

Figure 2.12 *Surface force measurements conducted between a PS sphere and plate in the presence of different concentrations of $C_{14}TACl$: in water, C=1.0 mN/m and D=4.4 nm, $\varphi_{0=}$ -32mV; at 8×10^{-5} M $C_{14}TACl$,, C=3.2 mN/m and D=4.6 nm, $\varphi_{0=}$ -19mV;at 1×10^{-4} , C=3.4 mN/m and D=8.0 nm, $\varphi_{0=}$ -4.6mV; at 5×10^{-4} , C=1.7 mN/m and D=4.0 nm, $\varphi_{0=}$ 46mV.*

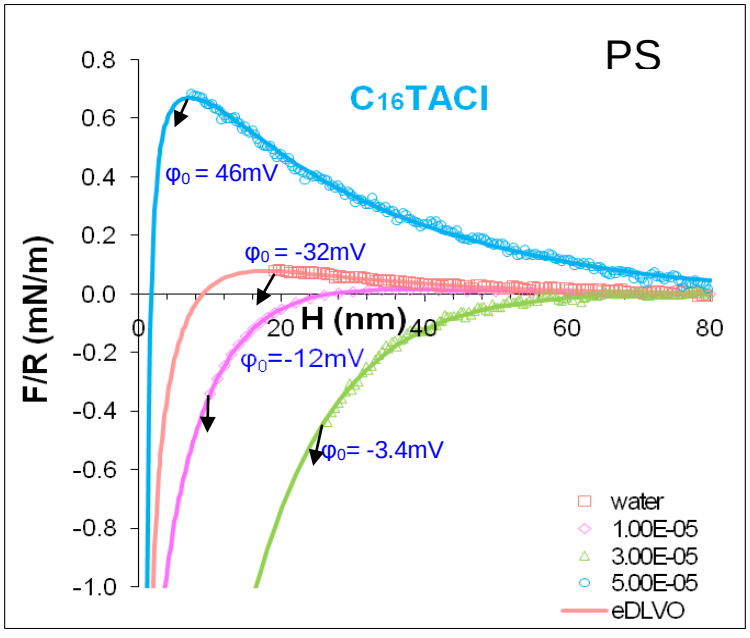

Figure 2.13 *Surface force measurements conducted between a PS sphere and plate in the presence of different concentrations of $aC_{16}TACl$: in water, C=1.0 mN/m and D=4.4 nm, $\varphi_{0=}$ -32mV; at 1×10^{-5} M,, C=3.4 mN/m and D=5.3 nm, $\varphi_{0=}$ -12mV;At 3×10^{-5} , C=3.7 mN/m and D=10.7 nm, $\varphi_{0=}$ -3.4mV; at 5×10^{-5} , C=1.1 mN/m and D=3.8 nm, $\varphi_{0=}$ 46mV.*

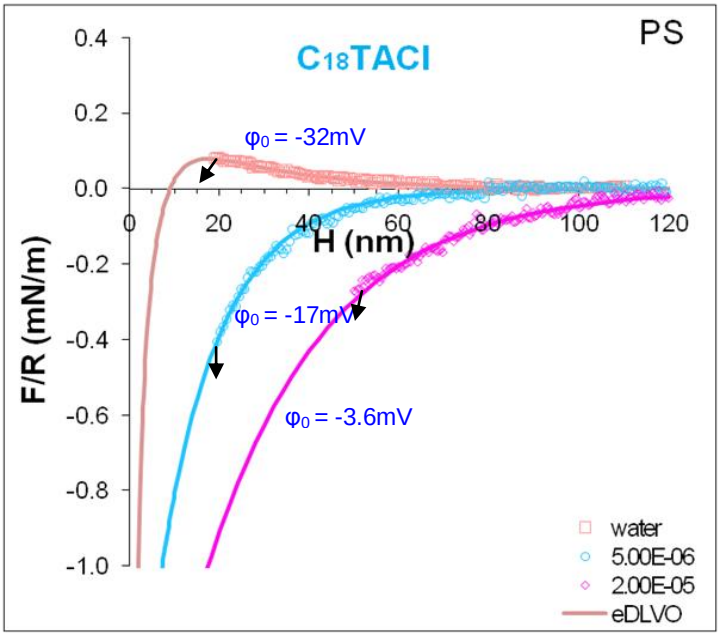

Figure 2.14 *Surface force measurements conducted between a PS sphere and plate in the presence of different concentrations of a C_{18}TACl: in water, C=1.0 mN/m and D=4.4 nm, $\varphi_{0=}$ -32mV; at 5×10^{-6} M C_{18}TACl,, C=3.3 mN/m and D=10.4 n, $\varphi_{0=}$ -17mV;at 2×10^{-5} , C=3.5 mN/m and D=12.4 nm; $\varphi_{0=}$ -3.6mV.*

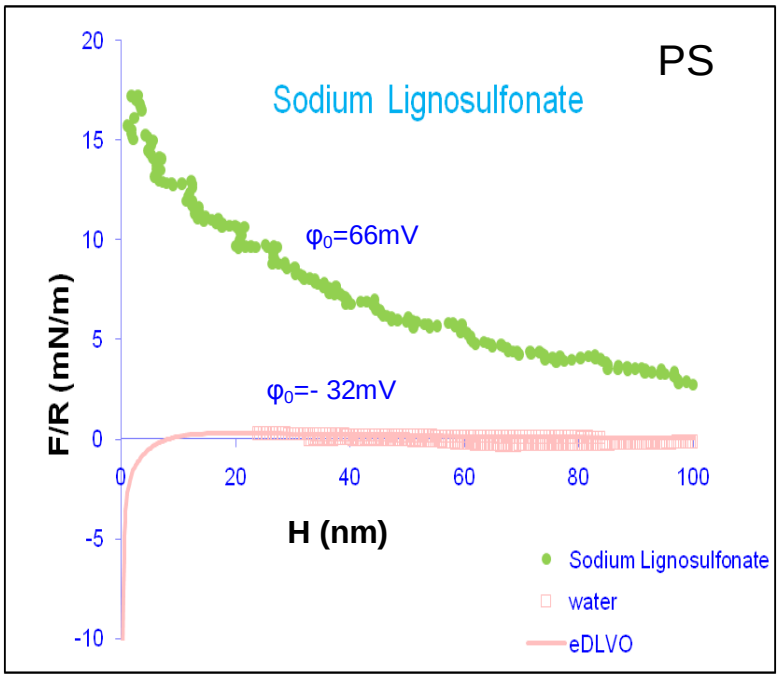

Figure 2.15 *AFM surface force measurements conducted between a PS sphere and plate in 0.1% sodium lignosulfonate solution: in water, C=3.1mN/m and D=7.6 nm, $\varphi_{0=}$ -32mV; at 0.1% sl. solution, $\varphi_{0=}$ 66mV.*

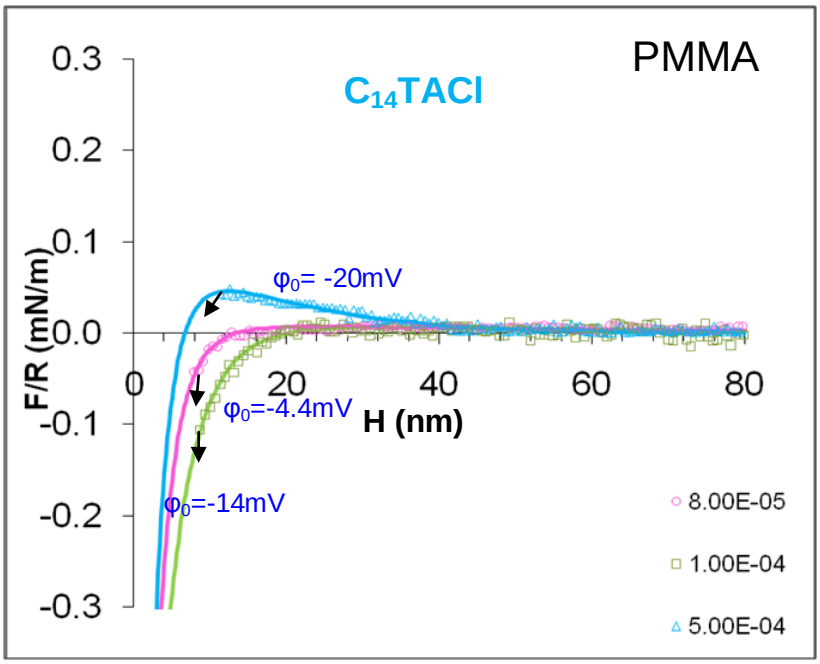

Figure 2.16 *Surface force measurements conducted between a PMMA sphere and plate in the presence of different concentrations of $C_{14}TACl$: in water, C=3.0 mN/m and D=4.0 nm, $\varphi_{0=}$ -68mV; at 8×10^{-5} M $C_{14}TACl$,, C=3.3 mN/m and D=4.3 nm, $\varphi_{0=}$ -14mV;at 1×10^{-4} , C=3.5 mN/m and D=4.9 nm, $\varphi_{0=}$ -4.4mV; at 5×10^{-4} , C=3.0 mN/m and D=4.1 nm, $\varphi_{0=}$ -20mV.*

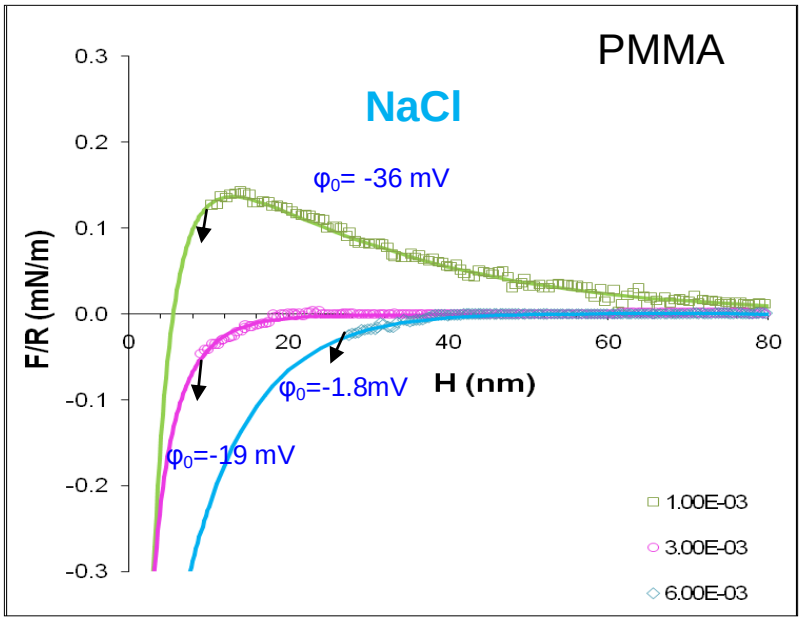

Figure 2.17 *Surface force obtained between PMMA sphere and plate in salt solutions: in water, C=3.0 mN/m and D=4.0 nm; $\varphi_{0=}$ -68mV;at 1×10^{-3} M NaCl, C=3.1mN/m and D=4.1 nm, $\varphi_{0=}$ -36 mV; at 3×10^{-3} , C=3.4 mN/m and D=4.5 nm, $\varphi_{0=}$ -1.8 mV; at 6×10^{-3}, C=3.6 mN/m and D=5.1 nm $\varphi_{0=}$ 3.6 mV.*

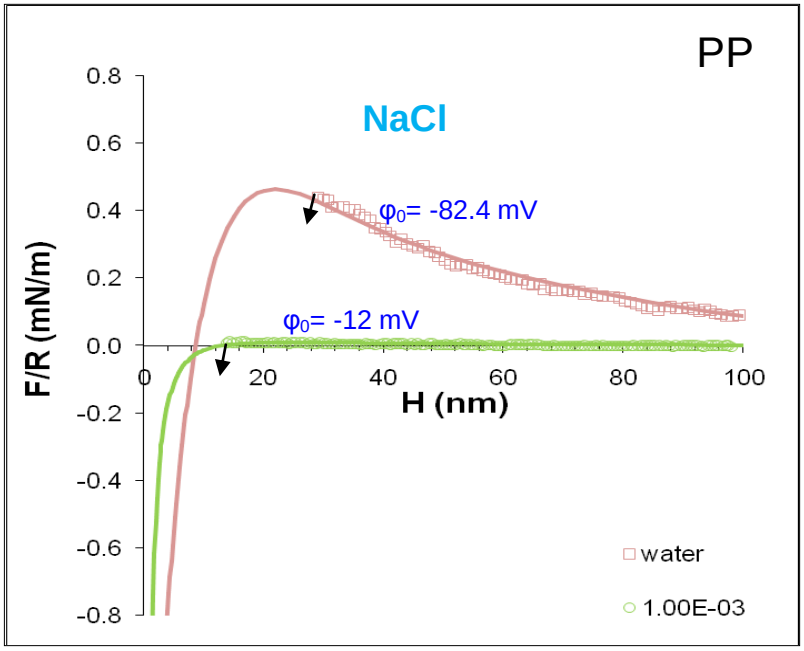

Figure 2.18 *Effect of NaCl on the surfaces forces measured between PP sphere and PP-coated substrate (silicon wafer) immersed in a 10^{-3} M NaCl solution: In water, C=3.1mN/m and D=7.6 nm; $A_{131}=1.05\times10^{-20}$ J; $\varphi_{0=}$ -82.4 mV; at 10^{-3} M NaCl, C=3.0 mN/m and D=8.1 nm, $A_{131}=1.05\times10^{-20}$ J; $\varphi_{0=}$ -12 mV.*

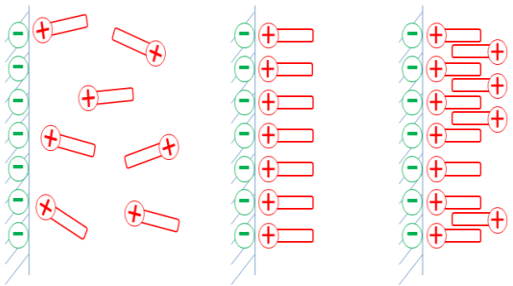

Figure 2.19 *Surfactant reverse orientation.*

Table 2.1 *Hydrophobic Force Constants of PS, PMMA PP and Teflon*

Polymers	**A_{131} (J)**	**Potential (mV)**		**θ (deg)**	**C (mN/m)**	**D (nm)**
		φ_0	ξ			
PS	$1.3x10^{-20}$	-32	-30	76	1	4.4
PMMA	8.0×10^{-21}	-68	-67	72	3	4
PP	1.05×10^{-20}	-82.4	-80	98	3.1	7.6
Teflon	3.59×10^{-21}	-86	----	110	3	5.6

Table 2.2 *Effect of $C_{14}TACl$ concentration on the hydrophobicity (θ) and decay length (D) of PS*

Surfactant	Concentration of $C_{14}TACl$	θ (degree)	$\varphi_{0\,(mV)}$	*C (mN/m)*	*D* (nm)
$C_{14}TACl$	0	76	-32	1.0	4.4
	8×10^{-5} M	84	-19	3.2	4.6
	1×10^{-4} M	96	-4.6	3.4	8.0
	5×10^{-4}M	78	46	1.7	4.0

Table 2.3 *Effect of NaCl concentration on the hydrophobicity (θ) and decay length (D) of PMMA*

Salt	Concentration of NaCl	θ (degree)	$\varphi_{0\,(mV)}$	*C (mN/m)*	*D* (nm)
NaCl	0	72	-68	3.0	4.0
	1×10^{-3} M	78	-36	3.1	4.1
	3×10^{-3} M	82	-1.8	3.4	4.5
	6×10^{-3}M	89	-19	3.6	5.1

.

III – SEPARATION OF MIXED PLASTICS BY FLOTATION

This chapter is devoted to the study of plastics floatation. Plastics are naturally hydrophobic and thus difficult to separate directly. However, adding surfactant can change their surface property and form different hydrophilicity, which makes froth floatation of plastics possible. As an indicator of wettability, the contact angles of two commonly used plastics, PS and PVC, were measured in the presence of various wetting agents. The objective of this study is to explore the efficiency of wetting agents for froth floatation of plastics.

3.1 Materials and Experiments

3.1.1 Plastics

PS sheets were obtained from United States Plastic Corporation, Lima, Ohio. PVC sheets were obtained from Polysciences, Inc., Warrington, PA. After being washed with plenty of water, plastic sheets were cut into 2×2cm pieces, and each piece was tied with a copper wire onto a glass for contact angle measurement

3.1.2 Surfactants

Five different surfactants were used wetting agents for the plastics. Dioctyl sodium sulfosuccinate (DSS) and Bij30 were purchased from Sigma Aldrich. Methyl cellulose (MC), sodium lignosulfonate (SL) and saponin were purchased from Fisher Scientific.

DSS, Bij30, SL and saponin solutions of the following concentrations, i.e., 0.01, 0.05, 0.1 0.15, 0.2, 0.25 and 0.3, were prepared by mixing 0.01, 0.05, 0.1, 0.15, 0.2, 0.25, 0.3 g of a surfactant with 100ml of water. MC solutions of concentration 0.01, 0.05, 0.1 0.15, 0.2, 0.25 and 0.3, were prepared by heating 100 ml of water to 90C° in a beaker, before adding 0.01, 0.05, 0.1, 0.15, 0.2, 0.25, 0.3g of solid MC. The solutions thus obtained were then cooled down under constant stirring.

The plastic samples, prepared as described in paragraph 3.2.1, were dipped in surfactant solutions for one hour. Contact angle measurements were then conducted using the contact angle goniometer FTA 200.

3.1.3 Water

Pure water was obtained by using the Direct-Q 3 (Barnstead IA) water purification system. The conductivity of the water was 18.2 MΩ/cm at 25°C and the surface tension was 72.5 mN/m at 22 ℃. The pure water was not purged with nitrogen gas to exclude the atmospheric CO_2. Thus; the pH of the water was within the 5.6-5.8 range.

3.1.4 Contact Angle Measurement and Captive Bubble Technique

A plastic sheet was immersed in a solution, and an air bubble, generated by pushing air through a syringe with a curved needle, was brought to contact with the solid sample from below. The contact angle was measured through the aqueous phase by means of a goniometer. More detailed procedure already been described in Chapter II.

3.1.5 Micro-flotation

Micro-flotation tests were conducted with various plastics powder in the presence of different wetting agents. The flotation experiments were performed on individual plastics rather than mixtures thereof.

3.1.5.1 Reagents

A 0.01% saponin solution (1g in 100 ml water) was used as a wetting agent to control the wettability (contact angle) of plastics, while MIBC (4-Methyl-2-pentanol)from Sigma Aldrich (98% purity) was used as frother. Both reagents were of commercial grade and used without further purification. Stock solutions of these reagents were prepared each day. All flotation tests were conducted using pure water at pH 5.6.

3.1.5.2 Test Procedure:

1g of plastic powder (which was purchased from Fisher Scientific) was fed into an 80 ml flotation cell and mixed with 60 ml of water. A glass stirring bar was used to agitate

the mixture. 6 ml of collector and a drop of frother were then added. The plastic suspension thus obtained was aerated for 3 min in order to completely mix the test sample with the reagents. While the plastic suspension was being aerated, the flotation froth was continuously removed. The concentrates obtained through flotation were dried in an oven for 1 hour. The flotation recovery was calculated by comparing the weight fraction of the plastic powder present at the beginning of the floatation test. All experiments were carried out at the natural water pH, and at room temperature.

3.2 Results

The separation of plastics by flotation was based on hydrophobicity (or wettability) control. Therefore, it was essential to characterize plastics in terms of their hydrophobic properties or contact angles. In the present work, the contact angle measurements were conducted on PS and PVC using both the sessile drop and the captive bubble techniques. Contact angles were initially measured on virgin polymers in the absence of any wetting agent using the sessile drop technique. The sessile drop contact angles measured on PS and PVC plates were 74.5 °and 70.8 °, respectively.

3.2.1 Effect of Different Wetting Agents on Contact Angles of PS

3.2.1.1 SL, DSS, Saponin and MC

The contact angle values of PS in the presence of different wetting agents are given in Table 3.1. In general, when using Sodium Lignolsulfonate(SL), Dioctyl sodium sulfosuccinate (DSS), saponin and methyl cellulose (MC) the contact angles decreased with increasing surfactant concentration. The largest change in contact angle was obtained with DSS as a wetting agent. The contact angle dropped from 74.4 °to 8.0 °as the concentration was increased from 0 to 0.3%. The case of saponin, however, it was particularly interesting: even though the smallest achievable contact angle was higher than with DSS, a significantly large decrease in contact angle was obtained at concentrations as low as 0.01%. Figure 3.1 shows the variation of the PS contact angle as a function of the surfactant concentration.

Table 3.1 *Effect of different wetting agents on PS contact angle*

Suarfactants	Concentration (% wt)							
	0	0.01	0.05	0.1	0.15	0.2	0.25	0.3
SL	74.4	63.6	39.2	31.9	31.3	30.5	29.9	29.4
DSS	74.4	73.0	72.1	23.5	15.0	13.0	11.0	8.03
Saponin	74.4	26.7	26.1	25.0	24.8	24.5	24.2	24.0
MC	79.1	67.2	47.7	37.6	37.3	36.9	36.5	36.2

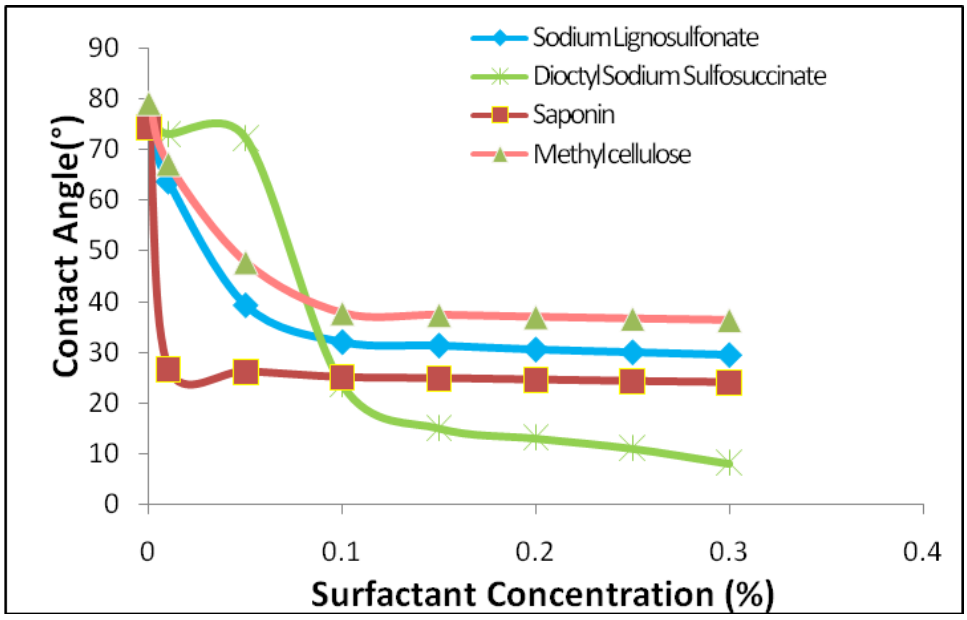

Figure 1.1 *Effect of different wetting agents on PS contact angle*

3.2.1.2 Effect of pH

Table 3.2 shows the contact angles of PS obtained at different pH. As shown the contact angle decreases with increasing pH. The results given in Table 3.2 have been plotted in Figure 3.2.

Table 3.2 *Effect of pH on PS contact angle*

pH	3.48	5.0	6.8	8.3	9.87	10.01
Contact Angle	110.15	100.00	90.00	86.10	82.57	81.60

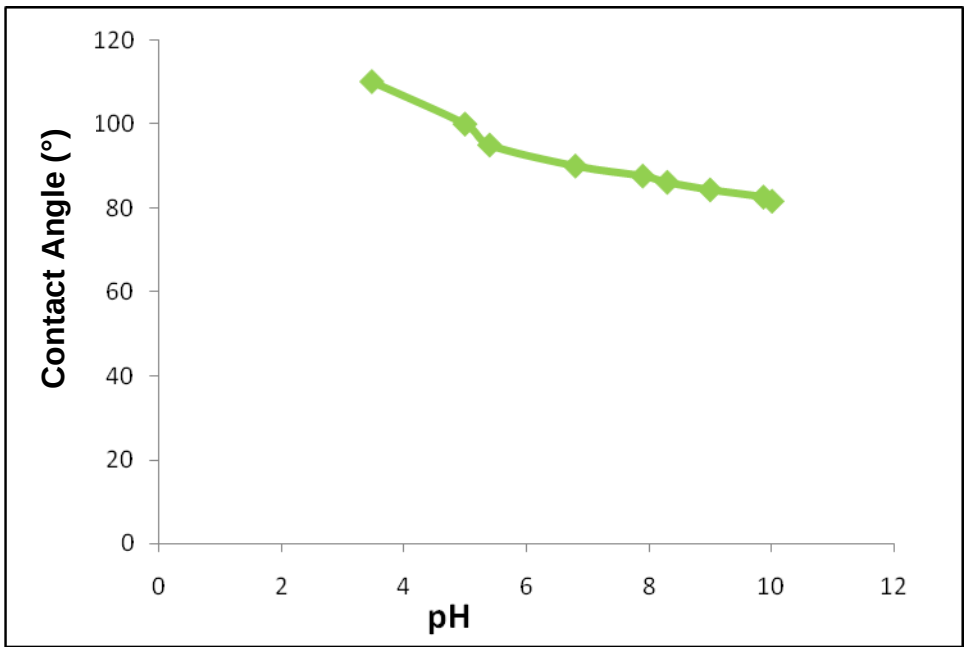

Figure 3.2 *Effect of pH on PS contact angle*

3.2.1.3 Effect of Bij 30

The PS contact angle values obtained with increasing concentration of Bij 30, a non-ionic surfactant, are presented in Table 3.3. A slight, non-significant decrease in contact angle is noticed as the surfactant is introduced. Figure 3.3 shows the variation of PS contact angle with respect to Bij 30 concentration.

Table 3.3 *Effect of non-ionic surfactant on PS contact angle*

Concentration	0	4×10^{-4}	1×10^{-3}	3×10^{-3}	5×10^{-3}
Contact angle	74.92	72.76	71.00	71.84	72.48

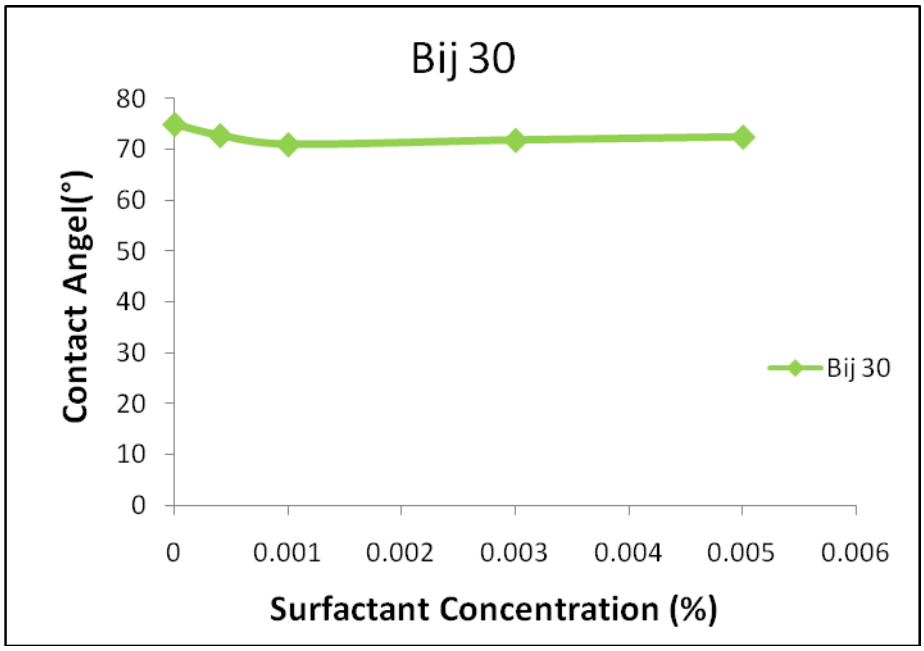

Figure 3.3 *Effect of non-ionic surfactant on PS contact angle*

3.2.2 Effect of Different Wetting Agents on Contact Angles of PVC

The contact angle values of PVC in the presence of different wetting agents and concentrations are given in Table 3.4. With SL, DSS, and saponin, the contact angles decreased with increasing surfactant concentration. The largest change in contact angle was obtained when using SL as a wetting agent. The contact angle dropped from 70.8 °to 3.0 °as the concentration was increased from 0 to 0.3%. Figure 3.4 shows the variation of PVC contact angles with changing surfactant concentrations. The reason that the large decreasing of the contact angle is because saponin adsorbs with the hydroxyl groups pointing toward the aqueous phase and the hydrophobic part in contact with the PVC.

Table 3.4 *Effect of different wetting agents on PVC contact angle*

Surfactants	Concentration (%wt)							
	0	0.01	0.05	0.1	0.15	0.2	0.25	0.3
SL	70.76	29.96	15.00	6.12	3.90	3.50	3.22	3.00
DSS	70.76	29.50	16.35	14.57	13.00	11.56	10.04	9.35
Saponin	70.76	36.47	57.48	73.93	76.41	77.20	77.56	78.59

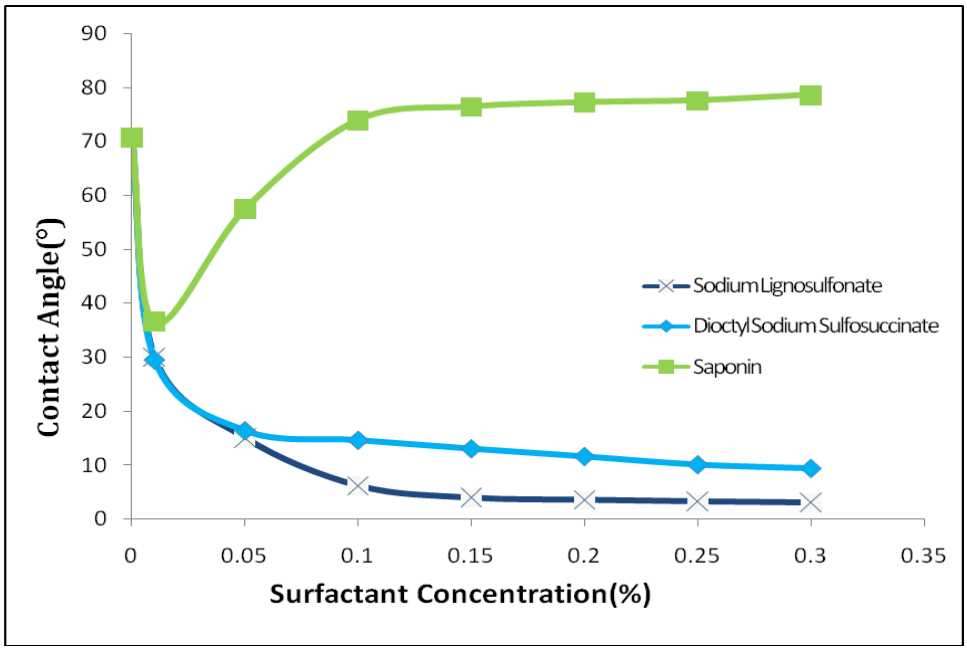

Figure 3.4 *Effect of different wetting agents on PVC contact angle*

3.2.3 Effect of Different Wetting Agents on Contact Angles of PS and PVC

3.2.3.1 Sodium Lignosulfonate (SL)

The contact angles of PS and PVC, obtained with increasing concentration of SL, are given in Table 3.5 and plotted in Figure 3.5. As shown, SL appears to be more effective in wetting PVC than in wetting PS. At 0.3% surfactant concentration, the contact angle of PVC dropped to 3.0 º, whereas the contact angle of PS dropped only to 29.4 º.

Table 3.5 *Effect of sodium lignosulfonate on contact angles of PS and PVC*

Plastics	Concentration (%wt)							
	0	0.01	0.05	0.1	0.15	0.2	0.25	0.3
PS	74.40	63.68	39.25	31.98	31.30	30.50	29.97	29.43
PVC	70.76	29.96	15.00	6.12	3.90	3.50	3.22	3.00

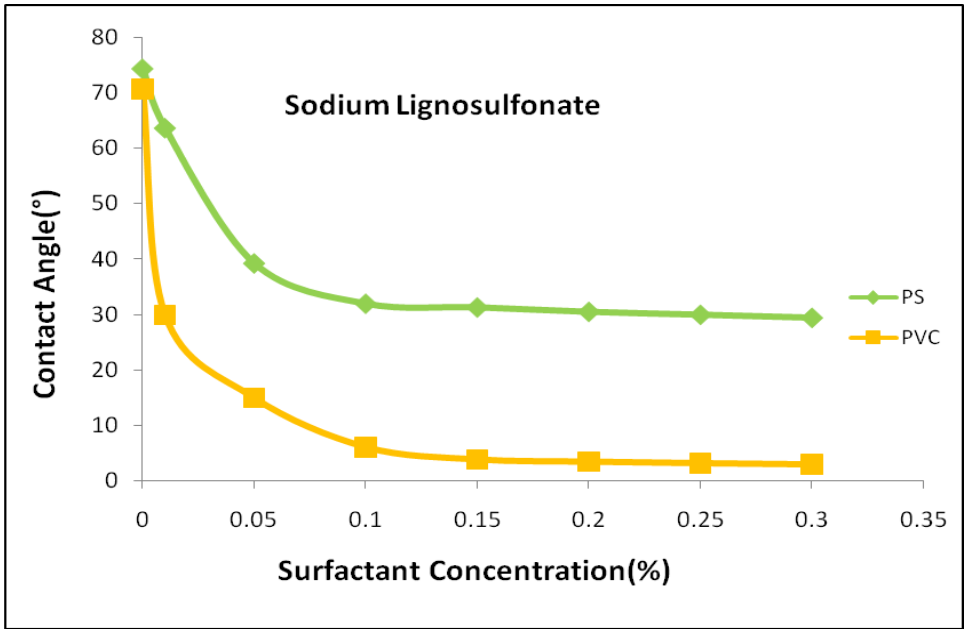

Figure 3.5 *Effect of sodium lignosulfonate on contact angles of PS and PVC*

3.2.3.2 Dioctyl Sodium Sulfosuccinate (DSS)

The contact angles of PS and PVC, obtained with increasing concentration of DSS, are listed in Table 3.6. For concentrations in the vicinity of 0.05%, DSS was much more effective in wetting PVC than in wetting PS; the PVC contact angle dropped from 70.8 º to 16.4 º, while the contact angle of PS remained unchanged. At higher concentrations, DSS performed similarly on both plastics. Figure 3.6 shows the variations of the PS and PVC contact angles with DSS concentration.

Table 3.6 *Effect of DSS on contact angles of PS and PVC*

Plastics	Concentration (%wt)							
	0	0.01	0.05	0.1	0.15	0.2	0.25	0.3
PS	74.40	73.00	72.19	23.54	15.00	13.00	11.00	8.03
PVC	70.76	29.50	16.35	14.57	13.00	11.56	10.04	9.35

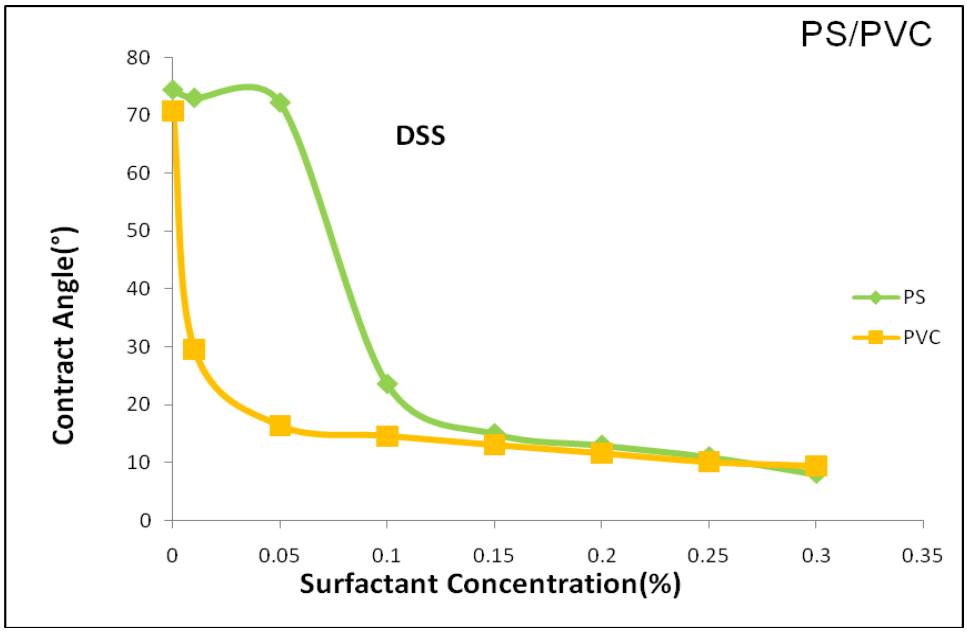

Figure 3.6 *Effect of DSS on contact angles of PS and PVC*

3.2.3.3 Saponin

The contact angles of PS and PVC, obtained with increasing concentration of saponin, are given in Table 3.7 and Figure 3.7. At concentrations above 0.05%, saponin became much more effective in wetting PS than in wetting PVC. The difference in contact angles between the two plastics became as large as 54 ºusing this surfactant as a wetting agent.

Table 3.7 *Effect of saponin on contact angles of PS and PVC*

Plastics	Concentration (%wt)							
	0	0.01	0.05	0.1	0.15	0.2	0.25	0.3
PS	74.40	26.75	26.16	25.00	24.80	24.05	24.20	24.00
PVC	70.76	36.47	57.48	73.93	76.41	77.20	77.56	78.59

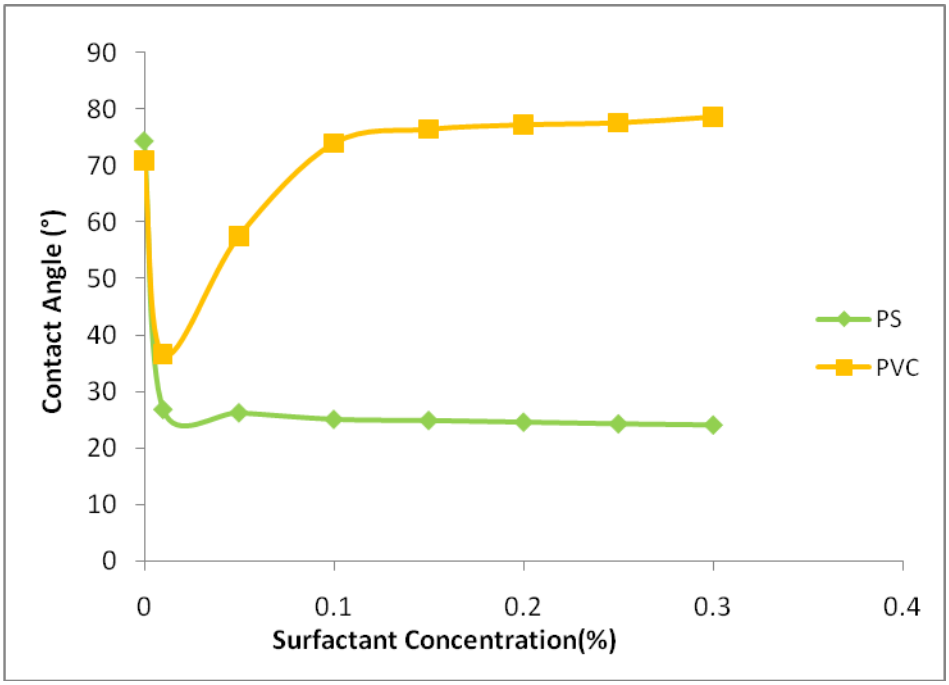

Figure 3.7 *Effect of saponin on contact angles of PS and PVC*

3.2.4 Flotation Test Results

According to the above result as shown in Figure 3.7, saponin at concentrations in excess of 0.05% is much more effective for wetting PS than PVC, suggesting that both plastics could be efficiently separated using this surfactant. Figure 3.8 shows the results of the micro-flotation test results conducted on PVC, PMMA, PP and PS using saponin as a wetting agent. As expected, the PVC recovery was almost complete at higher saponin concentrations, while the PS recovered was only 30% at 0.5% saponin. Therefore, saponin, as a wetting agent, appears to be a good candidate for the separation of PS from

PVC through flotation. However, the PP recovery was considerably higher than those of PS and PMMA.

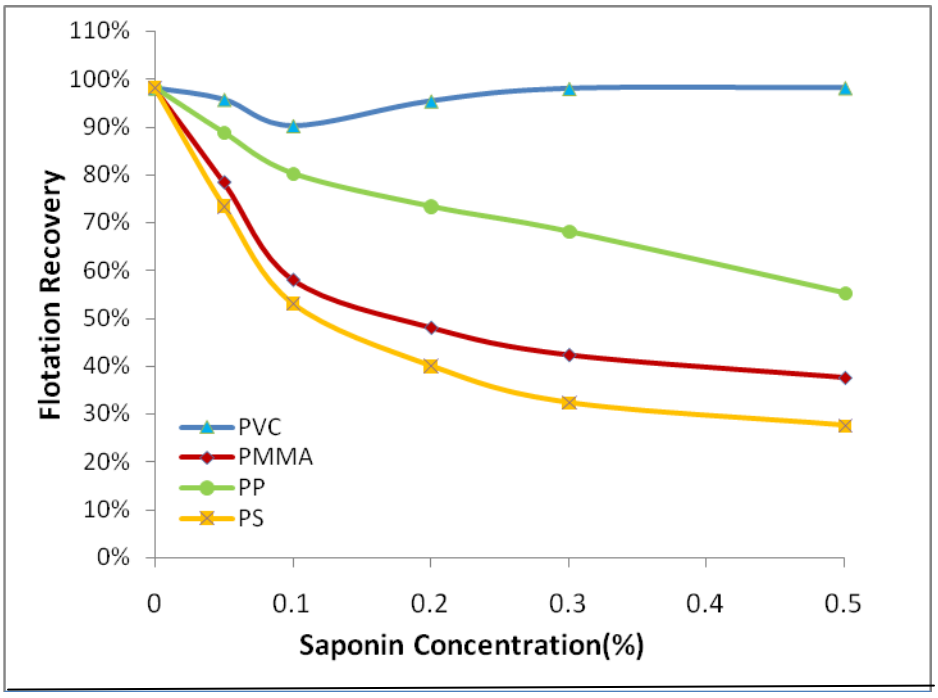

Figure 3.8 *Flotation recovery rates with respect to saponin concentration, for different plastics*

3.3 Summary

Separation of plastics by flotation is based on the control of hydrophobicity. Therefore, it is essential to characterize plastics in terms of their hydrophobic properties, which are directly related to their contact angles. Both the sessile drop and the captive bubble techniques were used in this work.

Flotation tests were conducted on PS and PVC, the separation of the two is important in the plastics recycling industry. The flotation tests were conducted using different wetting agents, including sodium lignosulfonate, DSS, MC and Saponin. All of these surfactants were shown to be effective in decreasing the contact angle and hence

suppressing the flotation. The flotation results showed that PVC can be readily separated from PS using saponin as a selective wetting agent.

REFERENCES

[1] B. V. Derjaguin, S. S. Duhkin, Trans. Inst. Min. Metall. 1961, 70, 221.

[2] J. Laskowski, J.A. Kitchener, J. Colloid Interface Sci. 1969, 30, 391.

[3] T. D. Blake, J. A. Kitchener, J. Chem. Soc Faraday Trans. 1972, 68, 1435-1442.

[4] J. N. Israelachvili, R. M. Pashley, Nature, 1982, 300, 341.

[5] M.E. Karaman, L. Meagher, and R.M. Pashley, Langmuir Vol. 9, pp. 1220, 1993.

[6] Y. Q. Li, N. J. Tao, J. Pan, A. A. Garcia, and S. M. Lindsay, Langmuir Vol. 9, pp. 637-641, 1993.

[7] L. Meagher, and V.S.J. Craig, Langmuir Vol. 10, pp. 2736, 1994.

[8] F.-J. Schmitt, T. Ederth, P. Weidenhammer, P. Claesson, and H.-J. Jacobasch, J. Adhesion Sci. Technology Vol. 13, pp. 79, 1999.

[9] O.I. Vinogradova, G. E. Yakubov, and H.-J. Butt, J. of Chem. Phys. Vol. 114, pp. 8124-, 2001.

[10] R. F. Considine, R. A.Hayes, R. G. Horn, Langmuir 1999, 15, 1657-1659.

[11] J. Zhang, R.-H. Yoon, M. Mao, W.A. Sucker, Langmuir, 2005; 21, 5831-5841

[12] E. E. Meyer, Q. Lin, J. N. Israelachvili, Langmuir, 2005, 21, 256-259.

[13] S. J. Miklavic, D. Y. C. Chan, L. R. White, T. W. Healy, J. Phys. Chem. 1994, 98, 9022-9032.

[14] J. Zhang, R.-H. Yoon, J.C. Eriksson, Colloid and surfaces A: Physicochem. Eng. Aspects 300 (2007) 335-345

[15] G. Xu, R.-H. Yoon, J. of Colloid and Interface Science, vol.134, no.2, pp. 427-434

[16] K. Saitoh, J. Nagano, and S. Izumi, New separation technique for waste plastics, Resource Recovery and Conservation Vol. 2, pp. 127, 1976.

[17] E. A. Sisson, U.S. Patent No. 5120768, June 9, 1992.

[18] J. Shibata, S. Matsumoto, H. Yamamoto, E. Lusaka, and K. Pradip, Int. J. Miner. Process Vol. 48, pp. 127-134, 1996.

[19] B. P. Singh, Filtration & Separation Vol. 35, Issue 6, pp. 525-527, 1998.

[20] J. Drelich, T. Payne, J. H. Kim, and J. D. Miller, Polymer Eng. & Sci. Vol. 38, Issue 9, pp. 1378-1386, 1998.

[21] C. Le Guern, P. Conil, and R. Houot, Minerals Eng. Vol. 13 (1), pp.53-63, 2000.

[22] C. Le Guern, P. Baillif, P. Conil, and R. Houot, J. Materials Sci. Vol. 36, pp. 1547-1554, 2001.

[23] H. Shen, E. Fossberg, and R. J. Pugh, Resources, Conservation and Recycling Vol. 35, Issue 4, pp. 229-241, 2002.

[24] H. Shen, R. J. Pugh, and E. Forssberg, Colloids and Surfaces A: Physicochemical and Engineering Aspects Vol. 196, Issue 1, pp. 63-70, 2002.

[25] G. Dodbiba, N. Haruki, A. Shibayama, T. Miyazaki, and T. Fujita, Int. J. Miner. Process. Vol. 65, pp. 11-29, 2002.

[26] P. Basarova, L. Bartovska, K. Korinek, and D. Horn, J. Colloid and Interface Sci. Vol. 286, pp. 333-338, 2005.

[27] J. Nalaskowski, S. Veeramasuneni, J. Hupka and J. D. Miller, J. Adhesion Sci. Technol., Vol. 13, No. 12. pp. 1519-1533(1999)

[28] R. F. Considine and C. J. Drummond, Langmuir 2000, 16, 631-635

[29] H. Stevens, R.F. Considine, C.J. Drummond, R.A. Hayes and P.Attard, Langmuir 2005, 21, 6399-6405

[30] W. A. Ducker, T. J. Senden, and R. M. Pashley, Nature Vol. 353, pp. 239-241, 1991.

[31] W. A. Ducker, T. J. Senden, and R. M. Pashley, Langmuir Vol. 8, pp. 1831-1836, 1992.

[32] J. P. Cleveland, S. Manne, D. Bocek, and P. K. Hansma, Rev. Sci. Instrum Vol. 64, pp. 403-406, 1993.

[33] P. Sonasundaran, Arthur T. Hubbard, "Encyclopedia of Surface and Colloid Science," 2nd Ed. Taylor & Francis, 2006.

[34] J.N. Israelachvili, "Intermolecular & Surface Forces Second Edition," Academic Press, p. 315, 1992.

[35] J. Vial, and A. Carre, Int. J. Adhesion and adhesives Vol. 11, No. 3, 1991.

[36] J.L. Parker, V.V. Yaminsky, and P.M. Claesson, J. Phys. Chem. Vol. 97, pp. 7706, 1993.

[37] M.W. Rutland, and J.L. Parker, Langmuir Vol. 10, pp. 1110-1121, 1994.

[38] P. Kékicheff, and O. Spalla, Phys. Rev. Lett. Vol. 75, pp. 1851, 1995.

[39] H. K. Christenson, and P. M. Claesson, Adv. Colloid Interface Sci. Vol. 91, pp. 391- 436, 2001.